AD NUMBER
ADB255411
NEW LIMITATION CHANGE

TO
Approved for public release, distribution
unlimited

FROM
Distribution authorized to U.S. Gov't.
agencies only; Proprietary Info.; Agu 99.
Other requests shall be referred to US
Army Medical Research and Materiel Comd.,
Fort Detrick MD 21702-5012.

AUTHORITY

USAMRMC ltr, 19 Jan 2001.

AD_____

Award Number: DAMD17-96-1-6151

TITLE: Biophysical Studies of the Type 1 Repeats of Human
Thrombospondin-1 to Characterize the Structural Basis of
its Angiostatic Effect

PRINCIPAL INVESTIGATOR: Kristin G. Huwiler, MS.
                        Deane F. Mosher, M.D.

CONTRACTING ORGANIZATION: University of Wisconsin System
                          Madison, Wisconsin 53706

REPORT DATE: August 1999

TYPE OF REPORT: Final

PREPARED FOR: U.S. Army Medical Research and Materiel Command
               Fort Detrick, Maryland 21702-5012

DISTRIBUTION STATEMENT: Distribution authorized to U.S. Government
agencies only (proprietary information, Aug 99). Other requests
for this document shall be referred to U.S. Army Medical Research
and Materiel Command, 504 Scott Street, Fort Detrick, Maryland
21702-5012.

20000703 042

DTIC QUALITY INSPECTED 4

NOTICE

USING GOVERNMENT DRAWINGS, SPECIFICATIONS, OR OTHER DATA INCLUDED IN THIS DOCUMENT FOR ANY PURPOSE OTHER THAN GOVERNMENT PROCUREMENT DOES NOT IN ANY WAY OBLIGATE THE U.S. GOVERNMENT. THE FACT THAT THE GOVERNMENT FORMULATED OR SUPPLIED THE DRAWINGS, SPECIFICATIONS, OR OTHER DATA DOES NOT LICENSE THE HOLDER OR ANY OTHER PERSON OR CORPORATION; OR CONVEY ANY RIGHTS OR PERMISSION TO MANUFACTURE, USE, OR SELL ANY PATENTED INVENTION THAT MAY RELATE TO THEM.

LIMITED RIGHTS LEGEND

Award Number: DAMD17-96-1-6151
Organization: University of Wisconsin

Those portions of the technical data contained in this report marked as limited rights data shall not, without the written permission of the above contractor, be (a) released or disclosed outside the government, (b) used by the Government for manufacture or, in the case of computer software documentation, for preparing the same or similar computer software, or (c) used by a party other than the Government, except that the Government may release or disclose technical data to persons outside the Government, or permit the use of technical data by such persons, if (i) such release, disclosure, or use is necessary for emergency repair or overhaul or (ii) is a release or disclosure of technical data (other than detailed manufacturing or process data) to, or use of such data by, a foreign government that is in the interest of the Government and is required for evaluational or informational purposes, provided in either case that such release, disclosure or use is made subject to a prohibition that the person to whom the data is released or disclosed may not further use, release or disclose such data, and the contractor or subcontractor or subcontractor asserting the restriction is notified of such release, disclosure or use. This legend, together with the indications of the portions of this data which are subject to such limitations, shall be included on any reproduction hereof which includes any part of the portions subject to such limitations.

THIS TECHNICAL REPORT HAS BEEN REVIEWED AND IS APPROVED FOR PUBLICATION.

REPORT DOCUMENTATION PAGE

Form Approved
OMB No. 0704-0188

1. AGENCY USE ONLY *(Leave blank)*

2. REPORT DATE
August 1999

3. REPORT TYPE AND DATES COVERED
Final (1 Aug 96 – 31 Jul 99)

4. TITLE AND SUBTITLE
Biophysical Studies of the Type 1 Repeats of Human Thrombospondin-1 to Characterize the Structural Basis of its Angiostatic Effect

5. FUNDING NUMBERS
DAMD17-96-1-6151

6. AUTHOR(S)

Kristin G. Huwiler, MS.
Deane F. Mosher, M.D.

7. PERFORMING ORGANIZATION NAME(S) AND ADDRESS(ES)
University of Wisconsin
Madison, WI 53706

Email: khuwiler@students.wisc.edu

8. PERFORMING ORGANIZATION REPORT NUMBER

9. SPONSORING/MONITORING AGENCY NAME(S) AND ADDRESS(ES)
Commander
U.S. Army Medical Research and Materiel Command
Fort Detrick, Frederick, Maryland 21702-5012

10. SPONSORING/MONITORING AGENCY REPORT NUMBER

11. SUPPLEMENTARY NOTES

This report contains colored photographs

12a. DISTRIBUTION / AVAILABILITY STATEMENT

Distribution authorized to U.S. Government agencies only proprietary information, Aug 99). Other requests for this document shall be referred to U.S. Army Medical Research and Materiel Command, 504 Scott Street, Fort Detrick, Maryland 21702-5012.

12b. DISTRIBUTION CODE

13. ABSTRACT *(Maximum 200*

Thrombospondin-1 (TSP1) is a disulfide bonded trimer of 450kD; each monomer contains three type 1 repeats (T1Rs). TSP1 and fragments that include the T1Rs have several documented functions including a role as an inhibitor of endothelial cell growth and migration, as well as an inducer of apoptosis. The purpose of this study was to express, purify, and biophysically characterize the T1Rs. Recombinant baculoviruses were generated that express the three T1Rs in tandem (P123) and the third T1R (P3) as secreted histidine-tagged fusion proteins. Protein purity, molecular mass determination, and disulfide-bond content was determined using mass spectroscopy. Micro-heterogenity arising from differential glycosylation was determined by western blotting, HPLC, and mass spectroscopy. Circular dichroism was used to access secondary and tertiary structure as well as thermal stability. Fluorescence spectroscopy revealed that the conserved tryptophans were quenched and in a partial polar environment in the native state. The effect of TSP1 and the T1Rs on endothelial cell (EC) morphology and death was determined. The results indicate the T1R encodes an independently folding protein module with spectral properties dominated by the conserved tryptophans. The protein is heterogeneously glycosylated with C-linked and O-linked sugars. The T1Rs are not responsible for the apoptotic effect on Ecs.

14. SUBJECT TERMS Breast Cancer
Thrombospondin-1, Angiogenesis, Protein Structure, Properdin, Fluorescence Spectroscopy, WSXWS motif

15. NUMBER OF PAGES
65

16. PRICE CODE

17. SECURITY CLASSIFICATION OF REPORT
Unclassified

18. SECURITY CLASSIFICATION OF THIS PAGE
Unclassified

19. SECURITY CLASSIFICATION OF ABSTRACT
Unclassified

20. LIMITATION OF ABSTRACT
Limited

NSN 7540-01-280-5500

Standard Form 298 (Rev. 2-89)
Prescribed by ANSI Std. Z39-18
298-102

FOREWORD

Opinions, interpretations, conclusions and recommendations are those of the author and are not necessarily endorsed by the U.S. Army.

_____ Where copyrighted material is quoted, permission has been obtained to use such material.

_____ Where material from documents designated for limited distribution is quoted, permission has been obtained to use the material.

_XN_ Citations of commercial organizations and trade names in this report do not constitute an official Department of Army endorsement or approval of the products or services of these organizations.

_____ In conducting research using animals, the investigator(s) adhered to the "Guide for the Care and Use of Laboratory Animals," prepared by the Committee on Care and use of Laboratory Animals of the Institute of Laboratory Resources, national Research Council (NIH Publication No. 86-23, Revised 1985).

_✓_ For the protection of human subjects, the investigator(s) adhered to policies of applicable Federal Law 45 CFR 46.

_XN_ In conducting research utilizing recombinant DNA technology, the investigator(s) adhered to current guidelines promulgated by the National Institutes of Health.

_XN_ In the conduct of research utilizing recombinant DNA, the investigator(s) adhered to the NIH Guidelines for Research Involving Recombinant DNA Molecules.

_XN_ In the conduct of research involving hazardous organisms, the investigator(s) adhered to the CDC-NIH Guide for Biosafety in Microbiological and Biomedical Laboratories.

Kristin M Hurrle   8/27/99
PI - Signature   Date

IV. Table of Contents

V. Introduction

Thrombospondin-1 (TSP1) is a modular disulfide-bonded trimeric glycoprotein with an approximate molecular mass of 450 kDa (Figure 1). TSP1 is a multi-functional protein that is synthesized and secreted by various cell types where it becomes incorporated into the extracellular matrix (ECM), including in the mammary tissue. TSP1 modulates several roles including new blood vessel growth or angiogenesis. Considerable work over the last decade has demonstrated that TSP1 induces an angiostatic effect *in vivo* and *in vitro*. (1, 2, 3, 4, 5). Some of these studies have implicated sequences within the type 1 repeats (T1R) for the angiostatic effect of TSP1 (Figure 2). The purpose of this work was to recombinantly express, purify, and biophysically characterize the T1R of human TSP1. This work would serve as a starting point for understanding the function of the T1R and the (primary, secondary, and/or tertiary) structure necessary for its activity. The broad scope of the research concerns the use of angiostatic molecules to inhibit tumor induced blood vessel growth. The initial growth of a human tumor usually does not require a direct blood vessel supply. However, in its absence, a solid tumor is limited in size to a 1-2 mm diameter and the metastatic potential of the tumor is thwarted (6, 7). The switching of cells within the tumor to an angiogenic phenotype stimulates new blood vessel growth toward the tumor and is dependent on the balance between stimulators and inhibitors of angiogenesis in the ECM (8). In the past year and a half, much attention has been focused on the angiostatic proteins angiostatin (9, 10) and endostatin (11, 12) which have been shown in animal studies to shrink primary tumors and decrease metastases without signs of resistance. These proteins, like TSP1, hold great promise in clinical use both alone and in combination with traditional chemotherapies to shrink primary tumor masses, prevent micro-metastases from expanding, and thereby indefinitely prolong the time a patient remains free of detectable cancer.

VI. Body

A. Task 1: Express and Purify P12 using GELEX

1. Introduction to GELEX

Baculoviruses are a group of viruses that contain circular, double-stranded genomic DNA and are capable of infecting insect cells. The baculovirus system was chosen due to its ability to catalyze disulfide bond formation, promote post-translational modifications, and produce large quantities of recombinant proteins. Our lab has expressed various combinations of the type 1 repeats (T1Rs) as fusion proteins with the gelatin-binding domain of fibronectin (13). These

C

recombinant fusion proteins, termed GELEX fusions, allow for the affinity purification of the recombinant proteins from the conditioned media using gelatin agarose.

The GE-1 baculovirus transfer vector contains the following features: the " GAP1-5" deletion mutant of the amino terminus of rat fibronectin that codes for the fibronectin signal sequence (14), the plasma transglutaminase cross-linking site, and the gelatin-binding domain of fibronectin. The PCR amplified cDNA encoding P12 was cloned into the BstXI restriction enzyme site that is found between regions coding for the transglutaminase site and the gelatin binding domain.

I determined conditions to isolate the recombinant protein under native conditions. The process involved cleaving the recombinant fusion protein bound to gelatin agarose with trypsin. Since there is a trypsin sensitive site between the cloned recombinant protein and the gelatin binding domain in the intact fusion protein, cleavage with trypsin frees the cloned recombinant protein from the gelatin-binding domain. Purification involves incubating the clarified media in batch at room temperature with a specific volume of gelatin agarose based on the amount of recombinant protein found in the media (1ml of packed gelatin agarose per 0.5mg of fusion protein). The resin/media mixture was spun down and the resin was transfered to a column. The column was washed with 10 column volumes of 20mM Tris-Cl, 150mM NaCl, pH 7.5. The column was then washed with 20 column volumes of 50mM Tris-Cl, 150mM NaCl, 2.0 mM $CaCl_2$ pH 8.4. The amount of trypsin added was equal to 0.2% (w/w) of the fusion protein in 1.2 column volumes. The resin was mixed every 5 minutes and the digest proceeded for 25 minutes at room temperature. Column fractions were then collected in tubes containing soy-bean trypsin inhibitor (STI) agarose resin. The column fractions with the STI resin were incubated with mixing for 30 minutes and then pooled and poured through an empty column. The protease inhibitor pefabloc (Boehringer Mannheim) was added to a final concentration of 2mM.

2. Problems Encountered using GELEX

As was detailed in the original project, I used the GELEX system to express and purify the first and second type 1 repeats in tandem (P12). However, many problems were encountered in obtaining large quantities of highly purified material. Expression of the recombinant fusion was ~10ug/ml; however, approximately 60% of the mass was due to the presence of the gelatin binding domain which served as the fusion partner and allowed purification of the recombinant protein on gelatin-agarose. The second problem encountered was the removal of the gelatin-binding domain. Although I determined conditions to cleave >95% of the the fusion protein without cleaving in between the T1R modules, the removal of the contaminating gelatin-binding domain proved problematic. There was a small population of the gelatin-binding domain that eluted from gelatin agarose with P12 following trypsin treatment. This population of gelatin-binding domain would not rebind to gelatin agarose following trypsinization. Although other

6

C

types of chromatography were investigated to remove the contaminating protein, the main problems encountered were very low yields and the formation of multimers of the type 1 repeats. Proteins expressed as fusions in the GELEX system retain the transglutaminse cross-linking site following removal of the gelatin-binding domain with trypsin. The presence of multimers was noted for different proteins expressed as fusions in the GELEX system and is thought to be due to this cross-linking site. In addition, P12 always appeared as two closely spaced bands on reducing SDS-PAGE and Western blots. The differences between the two populations was not due to differences at the amino-terminus as determined by N-terminal sequencing. The biophysical studies I had proposed require large amounts of very pure protein. Upon complete characterization of the GELEX system, I found it to be unsuitable for the isolation of very pure and homogeneous recombinant protein that I required for biophysical studies. As explained below, expression of the type 1 repeats as His-tag fusions using the baculovirus system was initiated.

3. Criteria for Design of a New Protein Expression System

Due to the problems encountered with GELEX, a decision to express the type 1 repeats as a fusion protein with a series of six histidines (His-tag) was made. The use of His-tags for affinity purification is commonly used by labs, including those performing biochemical and biophysical studies. In addition, histidine tagged proteins have been successfully expressed in the baculovirus system and baculovirus transfer vectors containing these sequences are commercially available. There were three things I required of the baculovirus transfer vector. First, it must contain a signal sequence that would direct the recombinant protein into the endoplasmatic reticulum. Since each T1R is proposed to contain three disulfide bonds, the recombinant protein must pass through the secretory pathway. Second, I wanted the His-tag at the C-terminus of the recombinant molecule. The baculovirus system is a dying one and the possibility to obtain recombinant protein with premature termination exists. Therefore, placement of the His-tag at the C-terminus ensures that full length protein is selected for in the purification. The third requirement for the baculovirus vector stemmed from the desire to remove the His-tag from the purified recombinant protein. Since one of the goals of the project was to obtain diffraction quality crystals, I wanted as little extra coding sequence that might interfere with the crystallization process. There are, however, reports in the literature of crystals being obtained for His-tagged proteins (15). To remove the His-tag, I needed a protease site encoded 5' to the His-tag. Unfortunately, there were no commercially available baculovirus transfer vectors that incorporated these features. Therefore, the pCOCO baculovirus transfer vector was constructed based on these specifications.

C

4. Construction of pCOCO Baculovirus Transfer Vector

The pAcGP67A baculovirus transfer vector (Pharmingen) was chosen as the starting point. It contains the GP67 signal sequence 5' to the multiple cloning site (MCS). This signal sequence is under the control of the very strong polyhedrin promoter. The pAcGP67A vector was modified 3' to the MCS by the addition of a DNA sequence that encodes a thrombin cleavage site followed by a His-tag. The exact sequence for the cleavage site is shown in Figure 3. A PstI restriction site was incorporated between the coding region for the thrombin cleavage site and the His-tag.

The primers used to generate this fragment are shown in Figure 4A and are called COCO forward and COCO reverse. These two primers have a nineteen base pair overlap. They were denatured at 94°C and then allowed to anneal. Extension was accomplished with Deep Vent DNA polymerase (New England Bioloabs) at 70°C for 7 minutes. The fragment was purified and then digested with XbaI and PpuMI. The digested product was purified and ligated into the pAcGP67A MCS at the XbaI and PpumI sites. The resulting transfer vector is termed pAcGP67.COCO or pCOCO (Figure 3).

The cDNA for P123 and P3 were cloned into the XmaI and XbaI sites as described below in section VI.A.5. The resulting baculovirus transfer vector can be used to generate recombinant baculoviruses that express the cDNA as fusion protein. The fusion protein will be directed to the secretory pathway by the amino terminal GP67 signal sequence. The carboxy-terminus of the fusion protein (COCO) contains a thrombin cleavage site and a series of six histidines. The His-tag allows the recombinant protein to be readily purified on nickel-chelate resin while the thrombin cleavage site allows the His-tag to be subsequently removed.

5. Cloning hTSP1 Type 1 Repeats into pCOCO Baculovirus Transfer Vector

The sequences encoding P123 and P3 were amplified from hTSP1 cDNA by the polymerase chain reaction (PCR). The forward and reverse primers for P123 as well as the forward primer for P3 amplification are shown in Figure 4B. The reverse primer used to amplify P3 was the same as used for P123. The forward primers introduced an XmaI site while the reverse primer added an XbaI site. These PCR products were cloned into the XmaI and XbaI sites in the MCS of pAcGP67.COCO. The DNA sequences were verified for all constructs prior to the generation of recombinant baculoviruses. The resulting baculovirus transfer vectors were used to generate recombinant baculoviruses that express the cDNA as a secreted fusion protein with a His-tag at the C-terminus.

8

C

6. Generation of Recombinant Baculoviruses

Recombinant baculoviruses were generated using Baculogold (Pharmingen) linearized AcNPV viral DNA. Co-transfections into Sf9 cells with baculogold and P123.COCO or P3.COCO were performed using CellFectin (Gibco-BRL). Recombinant baculoviruses were cloned by plaque purification. High titer ($1\text{-}5 \times 10^8$ pfu/ml) virus stocks were prepared using Sf9 cells. A graphical representation of the fusions expressed and the expected sizes are shown in Figure 5.

7. Purification of P123

The fusion protein is directed to the secretory pathway by the amino terminal GP67 signal sequence. This allows the recombinant protein to be purified from the conditioned media. The carboxy-terminus of the fusion protein (COCO) contains a thrombin cleavage site and a series of six histidines. The His-tag allows the recombinant protein to be readily purified on nickel-chelate resin (NiNTA, Qiagen), while the thrombin cleavage site allows the His-tag to be subsequently removed. An outline of the **purification scheme** follows:

> Infect High 5 Cells @ 1×10^6 cells/ml with Recombinant Baculovirus.
>
> Incubate at 27°C for ~62 hours.
>
> Clarify Conditioned Media (CM) by centrifugation to remove Cell Debris.
>
> Incubate clarified CM in batch with NiNTA resin.
>
> Wash NiNTA resin with buffer containing 10mM Imidazole.
>
> Elute NiNTA Resin with buffer containing 250mM Imidazole.
>
> Pool Fractions containing Recombinant Protein.
>
> Dialyze Recombinant protein into Thrombin Reaction Buffer.
>
> Digest 1 milligram of Recombinant Protein with 2-4 units of Biotinylated Thrombin.
>
> Incubate digest at room temperature for ~18 hours.
>
> Remove Biotinylated Thrombin by incubating Digest with Streptavidin Resin.
>
> Incubate with NiNTA Resin to remove uncleaved recombinant protein.
>
> Dialyze into Tris-buffered saline, pH 7.5.
>
> Concentrate by Ultra-filtration.

Yields of 10-20ug of fusion per milliliter of conditioned media were obtained for P123.COCO. A representative 14% SDS-PAGE of P123.COCO NiNTA eluates (5ul/eluate) is shown in figure 6. The eluates were run under reducing conditions. The P123.COCO eluted from the Nickel resin within the first several column volumes and the P123.COCO protein migrated between the 18kDa and 24kDa markers, as expected.

The results from loading 10ug of P123, post-thrombin cleavage, on a 12-20% SDS-PAGE gel under reducing and non-reducing conditions are shown in Figure 7. P123 appears as a single band

C

of about 20kDa, the expected size, under reducing conditions. Under non-reducing conditions, P123 appears as several closely spaced bands of about 20kDa, as well as one or more closely spaced bands of approximately 40kDa. The multiple 20kDa and the 40kDa bands are consistent with the presence of intramolecular and intermolecular disulfide-bonded isomers, respectively. Our data is consistent with that observed for the protein properdin, which contains six T1Rs in tandem, and for which two or more closely spaced bands of the size of monomeric properdin were observed following non-reducing SDS-PAGE (16, 17, 18). The paper by Farries and Atkinson (17) concluded that the multiple band pattern observed by non-reducing SDS-PAGE was not due to N-linked glycosylation and could be due to alternative intra-molecular disulfide bonding. We also suggest this as one possibility, although we have observed the presence of O- and C-linked glycosylation for P123 (Section VI.H.1). We have confirmed the sequence of the P123 DNA clones and do not believe the multimers arise from a point mutation. In addition, I have confirmed by Western blotting the conditioned media that P123 is secreted from the cells as a monomer and a dimer. Therefore, the dimerization is not due to the purification process. Another recombinant protein (P3E123) that we have expressed in the baculovirus system also displays a multiple banding pattern and contains bands the size of dimeric molecules on non-reducing SDS-PAGE. The protein P3E123 is derived from hTSP1 and contains the third type 1 repeat, followed by the first, second, and third EGF-like repeats in tandem. It is interesting to note that we do not observe these possible disulfide isomers/multimers for the third T1R (P3) or for the three EGF-like repeats (E123). We are pursuing the origin and role of these multiple bands observed for P123 and P3E123.

8. Reasons for Altering the Purification Protocol for P3.COCO

The level of expression (1-2ug/ml) of P3.COCO was substantially lower than that obtained for P123.COCO even after examining more than 10 clones of P3.COCO and optimizing infection conditions. The lower level of expression of P3.COCO presented problems when scale-up was undertaken in order to purify milligram quantities of the P3.COCO. I have found that when the His-tagged protein is expressed at low concentrations, the protein fails to bind the nickel resin efficiently. In order to increase the strength of the interaction between the His-tag and the NiNTA, I initially tried raising the pH of the conditioned media to ~8.0 by dialysis. The pH of the conditioned baculovirus media is ~6.3. This process was not only tedious since I was working with at least 1 liter of conditioned media, but it also failed to improve the purification yields. The procedure that I determined to work consistently for P3.COCO involved the concentration of the conditioned media prior to incubation with the NiNTA. The protocol is described below.

10

C

9. Purification of the Third Type 1 Repeat (P3.COCO)

High 5 cells (BTI-TN-5B1-4) were grown at 27°C using SF900 II serum free media. For large scale production, four liter shaker flasks were used. Cells were infected at a density of $1x10^6$ cells/ml. A multiplicity of infection (MOI) of 2 was routinely used and the infection was allowed to proceed for ~62 hours.

Since P3.COCO is directed to the insect secretory pathway by the GP67 signal sequence, the first step in the purification procedure involves clarifying the conditioned media (CM). The insect cells are pelleted at ~8000xg for 10 minutes. The CM is carefully decanted from the cell pellet and imidazole, pH 6.7, is added to a final concentration of 10mM. PMSF is then added to a final concentration of 2mM.

The second step involves the concentration of the CM using ultrafiltration. Prior to concentration, the CM is filtered through Whatman No.2 filter paper which possesses a particle retention of 8μm. The filtered CM is then concentrated using an Amicon CH2S Spiral Wound Cartridge ultrafiltration system. The media is concentrated at least 10-20 fold. The concentrated media is then centrifuged at 15,000xg for 15 minutes. The remainder of the protocol is similar to that used for P123.COCO and is outlined below.

> Incubate clarified concentrated CM in batch with NiNTA resin.
> Wash NiNTA resin with buffer containing 10-20mM Imidazole.
> Elute NiNTA Resin with buffer containing 250mM Imidazole.
> Pool Fractions containing Recombinant Protein.
> Dialyze Recombinant protein into Thrombin Reaction Buffer.
> Digest 1 milligram of Recombinant Protein with 2-4 units of Biotinylated Thrombin.
> Incubate digest at room temperature for ~18 hours.
> Remove Biotinylated Thrombin by incubating Digest with Streptavidin Resin.
> Incubate with NiNTA Resin to remove uncleaved recombinant protein.
> Dialyze into Tris-buffered saline, pH 7.5.
> Concentrate by Ultra-filtration.

Yields of 1-2mg of fusion per liter of conditioned media were obtained for P3.COCO. A representative 18% SDS-PAGE of P3.COCO NiNTA eluates (5ul/eluate) run under reducing conditions is shown in figure 8. The P3.COCO protein eluted from the Nickel resin within the first several column volumes. The molecular weight and low molecular weight markers are on the left-hand side of the gel and the eluates are labeled 1 through 5. The P3.COCO protein migrates between the 6kDa and 14kDa markers, as expected. The results from loading 10ug P3, post-thrombin cleavage, on a 12-20% SDS-PAGE gel under reducing and non-reducing conditions are shown in Figure 7. P3 appears as at least three closely spaced bands of about 8 kDa under reducing conditions. The expected size of P3 is 7250Da. We have shown by a

11

C

combination of western blotting (section VI.H.1), mass spectroscopy (section VI.H.2), and HPLC (section VI.H.5), that P3 is heterogeneously glycosylated. We are confident that the origin of the multiple bands for P3 by reducing SDS-PAGE is due to heterogeneous glycosylation. Under non-reducing conditions, P3 appears as a diffuse single band of about 6 kDa. Although, not apparent in Figure 7, the non-reduced P3 migrates faster than the reduced sample.

10. N-terminal Sequencing of P123 and P3

The COCO fusion proteins are expressed with the 38 mino acid long GP67 signal sequence. In order to determine if the fusion proteins had the GP67 signal sequence removed at the predicted cleavage site and to determine whether the signal sequence site was homogeneous, N-terminal sequencing of P123 and P3 was initiated. Purified P123 and P3 proteins were denatured, reduced, and run on a 14% SDS-PAGE gel. The proteins were transferred to PVDF and the blot was stained with 0.1% Amido Black. The N-terminal sequencing was performed in the lab of Dr. Johan Stenflo, Lund University, Sweden. The sample underwent >10 cycles of sequencing. The P123 and P3 samples were determined to have homogeneous N-termini beginning at the anticipated amino acid, based on the predicted signal sequence cleavage site. The results are presented in Figure 9.

11. UV Wavelength Scans of Recombinant T1Rs

UV wavelength scans were routinely collected for purified recombinant proteins to access purity, determine concentration, and to determine the presence of aggregrated protein. The scans were collected in a dual beam UV spectrophotometer using quartz cuvettes of 1 cm pathlength. The proteins were dialyzed into the following buffer: 15mM Tris-Cl, 150mM NaCl, pH 7.5. Three sucessive scans from 240nm to 340nm at 100nm/min were collected and averaged for each protein as well as the buffer control. The standard deviation that resulted from averaging the three scans never exceeded 0.002 absorbance units for any spectra collected. All data were baseline corrected. Figure 10 shows the wavelength scans for P3 expressed in Hi5 cells (A), P3 expressed in Sf9 cells (B), and P123 expressed in Hi5 cells (C). The maximum wavelength of absorbance for all three proteins is between 282-283nm. The spectra are dominated by the three conserved tryptophans per T1R. Examination of the region between 320nm and 340nm indicates there are no signs of aggregation that would interfere with spectroscopic studies.

12

C

B. Task 2: Synthesize peptides derived from the TSP1 T1R sequences

1. Initial Reasons for synthesizing petides

The anti-angiogenic potential of TSP1 was first described by Noel Bouck and collegues (1). In this study, the authors found a tumor suppressor-dependent inhibitor of angiogenesis to be functionally and immunologically equivalent to a proteolytic fragment of TSP1, termed gp140. Intact human TSP1 and gp140 were shown to inhibit neo-vascularization *in vivo* and migration of ECs toward bFGF *in vitro*. TSP1 was subsequently shown to inhibit EC proliferation in response to bFGF (3), cord formation by cultured ECs (4), and lumen formation (4).

In order to localize the active regions of TSP1 responsible for its effect on ECs, Bouck and collegues tested proteolytic fragments of TSP1 (2). These authors showed that the 50/70kDa trimer inhibited neovascularization in rat corneas, and inhibited EC migration in response to bFGF. The 50/70 kDa trimer was thought to span the oligomerization, procollagen, T1R, and T2R modules. Further localization was done by Bouck and other investigators using peptides to sequences within this region. Peptides to the T1Rs were shown to block bFGF induced EC DNA synthesis, migration, and corneal neovascularization (2). Based on these studies, we proposed to study the recombinant T1Rs as well as two peptides, derived from the second T1R, to learn the structural features of the angiostatic activity. However, subsequent work from the Bouck lab (19) as well as work from our lab (13) have determined that the original peptides were active for reasons not reflective of the native state of TSP1 or the T1Rs. I will discuss this new data in more detail in Sections VI.B.2 and VI.E.1.

2. New Data Concerning Biological Activity of Peptides and of Recombinant T1Rs

Although the peptides showed anti-angiogenic activity, the concentrations required were approximatle 1,000-fold higher than the concentrations required of TSP1. The peptides required 20-50uM concentrations for activity, while TSP1 was active in the low nanaomolar range (<20nM). Over the years, this has been a concern since the activity attributed to the peptides could result from a contamination in the the preparation. Bouck and colleugues have now reported this to be the case and their work is discussed below.

The Mal II peptide, sequence shown below, is derived from the second T1R and was synthesized by Bouck and collegues with alanines (A) substituted for cysteines 1 and 2 that are naturally present in the T1R. Since their initial report (2) concerning the anti-angiogenic activity of the synthetic Mal II peptide, the authors have found variable activity for different preparations. Bouck and collegues have now extensively analyzed their peptide preparations and report that pure, homogeneous Mal II peptide is inactive in angiogeneisis assays (19). The original activity attributed to the Mal II peptide was due to the presence of contaminating peptides containing D-amino acids. Substitution of D-amino acids into positions Ser-4, Ser-5, or Ile-15 in Mal II

C

resulted in peptides that possessed anti-angiogenic activity in the low nanomolar range, as measured by *in vitro* and *in vivo* assays. In addition, the authors found that a short seven amino acid peptide containing a D-Isoleucine at postion 15 still retained activity.

Mal II peptide   S P W S̲ S̲ A S V T A G D G V̲I̲ T R I R

In summary, the peptides derived from the second T1R sequence do not possess anti-angiogenic activity. The substitution of D-amino acids confers anti-angiogenic potential to the peptide. The work of Dr. Panetti, discussed in section VI.E.1, demonstrates that the heparin-binding activity of peptides derived from the T1Rs is not shared by the native recombinant T1Rs (13). Therefore, it is difficult to determine if either set of peptide data (with or without D-amino acids) reflects the activity of the native T1Rs with regard to angiogenesis. However, my preliminary data of the effect of the native T1Rs on endothelial cell survival contrasts with the data using D-amino acid substituted peptides (20). The survival data is presented in Section VI.H.8. As this report will demonstrate, we have concentrated our efforts on a thorough understanding of the recombinant T1R proteins biochemically and have begun the functional characterization.

C. Task 3: Analysis of Secondary Structure Composition using Circular Dichroism

1. Far-UV Circular Dichroism of P3 and P123

The University of Wisconsin-Madison Biophysics Instrumentation Facility's AVIV 62 ADS circular dichroism spectrophotometer was used to monitor the far-UV CD signal for P3 and P123. The P3 and P123 samples were dialyzed against 10mM Potassium Phosphate, 100mM Sodium Chloride, pH 7.5. A quartz cuvette of pathlength 0.1cm was used for data collection. Spectra were collected at temperatures between 25°C-65°C. The CD spectra were obtained by scanning from 260nm to at least 200nm. A minimum of three scans per temperature were collected and averaged. All data were baseline corrected and converted to molar ellipticity, mean residue weight (Θ_{MRW}).

The far-UV CD spectra of a protein examines the secondary structure adopted by the protein backbone. Figure 11A and B shows the thermal denaturation of P3 and P123 monitored by CD in the far-UV. The proteins were equilibrated at each of the following temperatures: 25°C, 37°C, 45°C, 50°C, 55°C, 60°C, and 65°C. The spectra for P3 and P123 are marked by positive ellipticity that could be due in part to trp. The two positive signals are also seen in the complement protein properdin which contains six type 1 repeats in series (21). Positive CD signal in the far-UV has been noted for other proteins with predominantly β-sheet and β-turn secondary structure that contain aromatic clusters (22). The CD spectra for P3 and P123 at 25°C where deconvolved using

C

the program CDNN (version 2.0.3.188) to obtain estimates of the amount of secondary structural elements. A table below summarizes the percent secondary structure determined for P3. Although, the spectra for P3 and P123 are very similar, the program returned values in excess of 10% error for P123 making these results unreliable.

Secondary Structure	Percentage
α-Helix	3.4 %
β-Sheet	50.6 %
β-Turn	19.0 %
Random Coil	34.9 %
Total	107.9 %

The spectra at 25°C compared to that at 37°C for P3 or P123, are nearly identical. Therefore there is no change in secondary structure between 25°C and physiological temperature. Heating P3 or P123 causes a transition to a random coil conformation with the loss of secondary structure beginning at 45°C. As seen in Figure 11C, the far-UV CD spectra of P3 and P123 at 25°C plotted as molar ellipticity (mean residue weight) are very similar. The suggestion is that the overall secondary structure of the three modules in tandem is not significantly altered when compared to the single module.

2. Near-UV Circular Dichroism of P3 and P123

The University of Wisconsin-Madison Biophysics Instrumentation Facility's AVIV 62 ADS circular dichroism spectrophotometer was used to monitor the near-UV CD signal for P3 and P123. The P3 and P123 samples were dialyzed against 10mM Tris-Cl, 150mM Sodium Chloride, pH 7.5. A quartz cuvette of pathlength 1cm was used for data collection. Spectra were collected at temperatures between 25°C-65°C. The CD spectra were obtained by scanning from 340nm to 240nm. A minimum of three scans per temperature were collected and averaged. All data were baseline corrected and converted to molar ellipticity, mean residue weight (Θ_{MRW}).

The near-UV CD spectra of a protein examines the chirality of the aromatic residues and disulfide bonds. Figure 12A and B shows the thermal denaturation of P3 and P123 monitored by CD in the near-UV. The proteins were equilibrated at each of the following temperatures: 25°C, 37°C, 45°C, 50°C, 55°C, and 65°C. The spectra for P3 and P123 are marked by positive ellipticity. The peak centered about 280nm is due to the trps, since neither P3 and P123 have tyrosine.

C

The spectra at 25°C compared to that at 37°C for P3 or P123, are nearly identical. Therefore there is no change in the chirality of the trp residues between 25°C and physiological temperature. Heating P3 or P123 to 55°C eliminates the chirality of the trps. As seen in Figure 12C, the near-UV CD spectra of P3 and P123 at 25°C plotted as molar ellipticity (mean residue weight) are very similar in shape. However, P123 is approximately two-thirds the intensity of P3. There is an overall difference in the chirality of the 9 trps in P123 compared to the three trps in P3.

3. <u>Far-UV Circular Dichroism of P3 in the presence of DTT</u>

I investigated the effect of DTT on the far-UV CD signal of P3. The P3 sample was dialyzed against 10mM Potassium Phosphate, 100mM Sodium Chloride, pH 7.5. A quartz cuvette of pathlength 0.1cm was used for data collection. Spectra were collected at temperatures between 25°C-45°C. Dithiothreitol (DTT) was added to final concentration of either 2mM or 4mM. The CD spectra were obtained by scanning from 260nm to at least 200nm. A minimum of three scans were collected and averaged and all data were baseline corrected.

Figure 13A follows over time the denaturation of P3 at 25°C induced by disulfide bond reduction. The denaturation is similar to that induced by temperature, as seen in Figure 11A; however, the denaturation is slow and is incomplete after 90 minutes at 25°C in the presence of 2mM DTT. Figure 13B follows the denaturation in the presence of 4mM DTT with increasing temperature and time. The loss of secondary structure requires in excess of 3 hours at physiologic (37°C) or higher to reach completion. This contrasts with the more rapid effect of DTT on the shift in wavelength of maximum fluorescence emission described in section VI.D.2.

D. Task 4: Fluorescence Spectroscopy to Anaylze Environment of Conserved Trps

1. <u>Monitoring of Fluorescence and CD Signals of P3 and P123 with Increasing Temperature</u>

The University of Wisconsin-Madison Biophysics Instrumentation Facility's AVIV 62 ADS circular dichroism spectrophotometer was used to monitor the far-UV CD signal at 229nm and the total fluorescence emission when an excitation wavelength of 284nm was used. The P3 and P123 samples were dialyzed against 10mM Potassium Phosphate, 100mM Sodium Chloride, pH 7.5. A quartz cuvette of pathlength 0.1cm was used for data collection. The temperature was scanned from 25°C to 75°C. The temperature was increased in 2°C increments using a slope of 50°C/min and an equilibration time of 1 minute. All data were baseline corrected.

Figure 14 shows the dual monitoring far-UV CD signals and the total fluorescence emission with increasing temperature for P3 (A) and P123 (B). The effect of thermal denaturation on the secondary structure and the effect on the trps are thereby simultaneously monitored. Heating P3 or P123 from 25°C->75°C causes a decrease in the CD signal at 229nm and an increase in the total fluorescence emission. The maximum fluorescence intensity for P3 compared to P123 is achieved

C

at a higher temperature for P3. The decrease in flourescence intensity of P3 seen above 65°C is due to the temperature effect on the fluorescence of trp. The decrease in flourescence intensity of P123 seen above 59°C is due to the temperature effect on the fluorescence of trp and inter-module quenching. The unfolding of P3 and P123 monitored by CD appears to be cooperative. The melting temperature for P3 and P123 determined from the CD signal are approximately 55°C.

2. Fluorescence Emission Spectra of P3 and P123 under Native and Denaturing Conditions

The data were collected on an SLM 8000 spectrofluorometer using quartz cuvettes of 1cm pathlength. Four conditions for each protein were tested: Native, 10mM Tris-Cl, 150mM NaCl, pH7.5 (TBS); 10mM DTT in TBS; 6M Guanidine Hydrochloride in TBS; 6M Guanidine Hydrochloride and 10mM DTT in TBS. The temperature was held constant at 25°C. The protein concentration for P3 and P123 in each of the four conditions was held constant. The total absorbance at 280nm was below 0.1 O.D.. A minimum of three scans were collected and averaged per condition. In addition, the change in the maximum wavelength of emission was followed during a titration of P3 and P123 with DTT.

Figure 15A and B shows the fluorescence emission spectra of P3 and P123 under four conditions: Native, 10mM Tris-Cl, 150mM NaCl, pH7.5 (TBS); 10mM DTT in TBS; 6M Guanidine Hydrochloride in TBS; 6M Guanidine Hydrochloride and 10mM DTT in TBS. Under native conditions, the wavelength of maximum emission (λ_{max}) for P3 and P123 are very similar, 332-333nm (Figure 15C). The environment of the trps in P3 and P123 would be expected to be slightly non-polar based on this λ_{max}. Upon reduction of the disulfides with DTT or denaturation of P3 or P123 with 6M GuHCl, there is a large enhancement in total fluorescence and a large red-shift in λ_{max} (Figure 15C). The λ_{max} emission under these conditions is ~350nm which is indicative of the trps being fully solvent exposed. In the native conformation, the disulfides appear to act as quenchers and the trps are in a less polar environment compared to the denatured or reduced state.

Figure 15D shows the change induced in λ_{max} emission for P3 and P123 upon titration with DTT. The addition of 2-4 mM DTT resulted in the maximum change in λ_{max} emission. This change was completed within 20 minutes at room temperature. By monitoring the fluorescence it is clear that disulfide bond reduction alters the environment of the trps. As described above in section VI.C.3, I have investigated the effect of DTT on P3 secondary structure by monitoring the far-UV CD signal. Addition of 2mM DTT caused a slow loss of secondary structure. After 2.5 hours in 2mM DTT at 25°C, a wavelength scan in the far-UV revealed that P3 still retained some of its secondary structure. Heating the reduced P3 sample to 45°C in the presence of 4mM DTT for 3.5 hours resulted in near complete elimination of secondary structure. The fluorescence studies indicate that the disulfides strongly contribute to maintaining the environment of the trps

17

C

and the effect of reduction is seen in minutes of DTT addition. The CD studies show that the disulfides contribute to the thermal stability of the structure of P3 since lower temperatures will unfold the protein in the presence of DTT. However, the effect of disulfide bond reduction on secondary structure is slow at 25°C and takes hours to reach completion.

3. Determination if the Conserved Trps are Solvent Accesible or Buried in the Native State

We employed several strategies to determine that the three conserved trps (WXXWXXW) per T1R are solvent accessible. First, we obtained UV-absorbance difference spectra for theT1Rs in TBS or in TBS plus 20% glycerol. The presence of glycerol resulted in an enhancement in the absorbance and a shift to longer wavelengths for λmax. Alteration in the absorbance spectra by glycerol indicates that the trps are accessible to molecules of the size of glycerol (mean diameter of 5.2Å) (23). Second, the presence of C-linked glycosylation on the central trp (section VI.H.4) in the WXXWXXW motif indicates that the trps are not fully buried, but are in a solvent accessible environment. A partial mechanism for the enzyme catalyzed C-linked glycosylation is known and it involves the use of dolichyl-phosphate-mannose as the mannose donor(24). Third, the fluorescence λmax emission (Section VI.D.2) for P3 and P123 in the native state indicates that the trps are in a partially polar environment which is consistent with them being partially solvent accessible. The WSXWS motif found in the T1Rs is the most highly conserved sequence in the hematopoietic receptor superfamily (25). Several structures for members of this family have been solved (26, 27, 28). From these papers it is clear that the WSXWS motif contributes to an irregular β-bulge structural motif that involves the stacking of the indole side chanis of trp with hydrophilic side chains. These structures have determined that the β-bulge motif is solvent accessible and this data is consistent with our fluorescence data, absorbance data, and the fact that are proteins are modified on the central trp. Therefore, the effect of external quenchers was not pursued since we obtained data from several different methods indicating that the trps are partially solvent accessible.

E. Task 5: Effect of Heparin examined by Fluorescence

1. New Data Concerning Interaction of Heparin with the native recombinant T1Rs

The T1Rs, and other modules of TSP1, were expressed as GELEX fusions in our lab using the baculovirus sytem (Section VI.A.1). Dr. Tracee Panetti and collegues used these modules to determine the ability of native recombinant segments of hTSP1 to interact with heparin and fibrinogen/fibrin (13). The recombinant proteins used in this study were CP123, the procollagen, first, second, and third T1Rs; P123, the first, second, and third T1Rs; P12, the first and second T1Rs; P1, the first T1R; and P3, the third T1R. A table is provided below which summarizes this work with regard to the native recombinant proteins ability to bind heparin.

18

C

Recombinant Protein	0mM NaCl	50mM NaCl	150mM NaCl
CP123	+ + + +	+	-
P123	+ +	+	-
P12	+ + +	+	-
P1	-	-	-
P3	+	-	-

A summary of these findings with regard to P123 and P3 follows. P123 binds heparin in the absence of salt, but the binding is incomplete. Increasing the salt concentration, decreases the binding of P123 to heparin such that trace amouts bind in 50mM NaCl and none binds in 150mM NaCl. P3 performed more poorly than P123, since only trace amounts of P3 bound heparin at 0mM NaCl and none bound at either 50mM or 150mM NaCl.

It has been known for many years that the thrombin and chymotrypic fragments of TSP1 which contain the procollagen and T1Rs do not bind heparin, sulfatide, or proteoglycans in the presence of physiologic salt (150mM) (29, 30). The results of Dr. Panetti are consistent with these findings. However, they contrast with the papers illustrating that peptides derived from the T1Rs bind to heparin at 4°C in 150mM NaCl (31, 32) and the paper showing a reduced and alkylated endopeptidase fragment of TSP1 binds heparin (33). Therefore, the paper by Dr. Panetti *et al.* (13) illustrates the importance of utilizing native protiens to determine functional activity of segments of a large modular protein, since non-native fragments and small peptides can yield misleading information.

2. Effect of Heparin on P3 and P123

In light of this information, I used low salt conditions (10mM NaCl) when examining the effect heparin on the fluorescence properties of the T1Rs. The data were collected on an SLM 8000 spectrofluorometer using quartz cuvettes of 1cm pathlength. Two conditions for each protein were tested: 10mM Tris-Cl, 10mM NaCl, pH7.6; Heparin (50ug/ml) in 10mM Tris-Cl, 10mM NaCl, pH7.6. The temperature was held constant at 25°C. The protein concentration for P3 and P123 in each of the conditions was held constant (15ug/ml). The total absorbance at 280nm was below 0.1 O.D.. A minimum of three scans were collected and averaged per condition. There was no significant change (1nm) in the λ_{max} emission for P3 or P123 when heparin was present. There was no change in the fluorescence intensity for P3 and a very small increase in intensity for P123. The effect on the trp micro-environment of the T1Rs due to the presence of heparin was absent or very small.

19

C

F. Task 6: Effect of Heparin on the T1Rs examined by Circular Dichroism

The interaction of the T1Rs with heparin was studied by Dr Panetti, as discussed in Section VI.E.1. Only under conditions of no salt or low salt was a portion of P3 or P123 able to bind heparin. Therefore, it would be under these low salt conditions that any effect of heparin on the secondary structure or the chirality of the trps would be measurable. However, these experiments were not possible for solubility reasons. I have found the solubility of the T1Rs to be dependent on the salt concentration, such that increasing protein concentration in the absence of increased salt results in aggregation as measured by UV spectroscopy. Circular dichroism requires concentrated protein solutions that are free of aggregrates. In order to avoid protein aggregation in the CD experiments discussed in section VI.C, I required the presence of 100mM NaCl. Therefore, the effect of heparin on the T1Rs examined by CD was not feasible because these experiments required salt concentrations that prevented the T1Rs from binding heparin.

G. Task 7: Crystallography

Under the guidance of Dr. Ivan Rayment, University of Wisconsin-Madison, I performed a crystallization trial of the type 1 repeats using P12 expressed in the GELEX system. In order to grow crystals of diffraction quality, supersaturated solns of the proteins must be prepared so that the protein will slowly crystallize. Hanging-drop vapor diffusion using 102 different solutions was employed. Trials at room temperature and 4°C were set-up; however, no crystals were obtained from either temperature. Several possible reasons exist including the presence of "tails" on the GELEX construct, the use of a recombinant protein with two T1R modules, and the heterogenous glycosylation of the recombinant protein . The first reason listed above pertains to the "tails" on the GELEX recombinant proteins which are extra amino acids at the N- and C-termini that are part of the GELEX construct (Section VI.A.1). The extra amino acids are not part of the the T1Rs and are flexible, which could interfere with the crystallization process. The second reason involves the use of P12 for the crystallization trial. P12 is composed of the first and second T1R modules. If the linker segment between P1 and P2 is flexible, then it would be more difficult to crystallize the tandem T1R as opposed to a single module. The data presented in section VI.H. would indicate that the linker between P1 and P2 is flexible and solvent accessible at 37°C. The third reason and the biggest problem faced, in light of the biophysical data I have collected on the T1Rs expressed in the baculovirus system, is the heterogeneous C- and O-linked glycosylation. The C- and O-linked glycosylation is explained in detail in Section VI.H.4. The T1Rs were glycosylated when expressed in either the GELEX or COCO systems. Micro-heterogeneity, such as due to differential glycosylation, is a problem since it prevents uniform packing of the molecules and hence crystal growth. There is no convenient way to remove these types of glycosylation as would

20

C

be the case if the glycosylation was N-linked. I tried expressing the protein in the presence of the O-linked inhibitor benzyl N-acetyl-α-D-galactosaminide (Oxford glycosystems) and was unable to detect any product from a small scale purification, even though mass spectroscopic investigations (sections VI.H.1, 2 and 4) have proven that unglycosylated forms are released from the cells under normal infection conditions.

Several other options exist to try to obtain the structure of the T1Rs and are discussed below. First, investigators have found that expressing the protein of interest from a different species will allow crystals to be obtained. Subtle variation in surface amino acids can allow better packing or alter the solubility of the recombinat protein. A second option would be to express the T1R(s) in *E.coli* in order to reduce the likelihood of heterogeneous glycoforms. Thid, the T1Rs could be expressed using the baculovirus system and then purified by HPLC to isolate homogeneously glycosylated or unglycosylated forms. The separation of the glycoforms is discussed in section VI.H.6. However, expression in *E.coli* or the use of HPLC will require the refolding of the protein. I have found a way to refold P3 following thermal denaturation but not one for P123. Therefore, if the T1Rs were to be refolded for the purposes of structure determination, then the single P3 T1R would be recommended. A fourth option to solve the 3D structure would be to utilize NMR, which requires protein concentrations of 1-4mM. I have never been able to achieve these concentrations for the T1Rs. However, further variation in pH and salt could be undertaken. Through my studies with mass spectroscopy, I have determined that the protein is acid stable and perhaps a significant drop in pH (<5.5) would increase the solubility. If NMR was used for structure determination, then conventional 2-Dimensional methods would need to be employed for the following reason. Although 3-Dimensional methods for solving protein structures are common, it would require the uniform labeling of the protein. In the baculovirus system, the uniform labeling of recombinant proteins currently costs about $8,000 per liter. Since P3 is expressed at low levles (1-2mg/L), it would be cost prohibitive to express it as a labeled protein.

Although I have not been able to obtain diffraction quality crystals and hence solve the structure, I have elucidated several key features that pose problems and potential means that could be utilized in the future. Solving the structure of the T1Rs is an independent project that will benefit from the work I have done to characterize the recombinant proteins.

H. Additional Tasks Completed

1. Determination of Glycosylation in P3 and P123 by Western blotting

The DIG Glycan Detection system (Boehringer Mannheim) has been used to determine if baculovirally expressed P3 and P123 are glycosylated. The three step method employs an enzyme immunoassay to detect sugars on immobilized protein. The proteins were expressed in High 5 cells and purified as described previously. In addition, the positive control glycoprotein transferrin

C

and the negative control unglycosylated protein creatinase were run along side the recombinant T1Rs. The proteins were run on a 14% SDS-PAGE and transferred to nitrocellulose. Manufacturer's instructions for detecting glycosylation of immobilized proteins were followed. Figure 16 contains the Western blot and shows that both P3 and P123 expressed using the baculovirus system are glycosylated. Using the same system, I have determined that the fusion partner (GELEX or COCO) used during expression does not alter the glycosylation of P123.

2. Molecular Mass determination of P3 and P123 by MALDI-TOF

Both P3 and P123 proteins were extensively dialyzed against 5% acetic acid at 4°C and then lyophilized. The proteins were resuspended in water to a concentration of 10-40pmol/ul. The matrix was α-cyano-4-hydroxycinnamic acid at 10mg/ml. The data were collected on a Bruker matrix-assisted laser desorption ionization time-of-fight (MALDI-TOF) mass spectrometer (MS) at the University of Wisconsin- Madison, Department of Chemistry. Internal calibrants of insulin, ubiquitin, and/or trypsinogen were used to determine the masses.

Representative MALDI-TOF mass spectra of P3 and P123 are shown in Figure 17. The table in figure 17 summarizes the average mass of the peaks of P3 determined from greater than 10 independent measurements using insulin (5734.6Da) and ubiquitin (8565.9 Da) as internal calibrants. P3 appears has a minimum of 4 peaks which differ in mass by 154-176 Da. The mass of the first peak is 7254.3 ± 6 Da, which agrees with the expected mass of 7250 Da for P3 based on the known N- and C-termini and assuming the presence of three disulfide bonds. The mass difference between one peak and the next is on the order of the mass of a single sugar, ~162Da. Therefore, we thought it is possible that these mass differences are due to the sequential addition of single sugars to the P3 protein. As discussed in section VI.H.1, P3 appears to be glycosylated when analyzed using the DIG Glycan Detection system. I have attempted chemical removal of the carbohydrate with sodium borohyride, but the procedure resulted in complete fragmentation of P3. However, in colloboration with Dr. Jan Hofsteenge, Friedrich Miescher Institut, we have determined that the T1Rs contain mono- and disaccharide additions in the form of C- and O-linkages (section VI.H.4).

The mass determination of P123 has been more difficult than for P3. I have found it challenging to obtain good signal to noise ratios and well resolved peaks. As seen in figure 17, P123 appears as two poorly resolved peaks. It is likely that there are more peaks present than are visible. Due to the low signal and the relatively broad peaks, it has been difficult to accurately determine the mass for P123. The average mass of the first peak of P123 is ~19919 Da. The experimentally determined mass is 44 Da under the expected mass of P123 (19963 Da). This difference is twice the expected error for a protein this size, since the error is usually ±0.1% of the mass. The error is likely due to the poor resolution and poor signal obtained for P123 as well as

22

C

for the internal calibrant trypsinogen (23982 Da). The difference in mass between the two peaks observed for P123 is 159Da. Again, this is similar to what is seen for P3 and is on the order of the addition of a single sugar. I have tried to improve the resolution of the P123 MS data, by employing methods to remove trace ions that could interfere with MALDI-TOF MS and by using matrices other than α-cyano-4-hydroxycinnamic acid, but I have not consistently seen an improvement in the resolution of the data.

3. Determination of the Disulfide Bond Content of P3 using MALDI-TOF

Figure 18 summarizes the data obtained when the P3 protein was labeled with Iodoacetic acid (IA) under four conditions: Native, DTT treated, Guanidine Hydrochloride (GuHCl) treated, or DTT and Guanidine Hydrochloride (DTT/GuHCl) treated. This experiment is designed to determine if there are any free thiols present in P3 and the number of disulfide bonds. The table lists the mass of the first peak of P3 for each treatment condition. Only under reducing conditions, DTT or DTT/GuHCl, were cysteines labeled with IA. The number of cysteines labeled is determined by dividing the change in mass due to labeling by the mass of the label (IA). For both reducing conditions, 6 cys were labeled which is the number of Cys present in P3. Since denaturing P3 in 6M GuHCl and labeling with IA failed to cause a mass shift, there are no free thiols present. In addition, the control experiment verified that there were no cystines present that resulted from a bond between cys in P3 and a small molecule containing cys. Therefore, all the cys in P3 are in disulfide bonds. I have also tried this experiment with P123; however, I obtained poor resolution of the data. As mentioned above, I have worked on improving the resolution with the native protein.

4. C-linked Glycosylation as well as O-linked Glycosylation of P3 and P123

Dr. Jan Hofsteenge has published numerous papers on the relatively new form of glycosylation termed, C-mannosylation, which involves the attachment of an α-mannosyl residue through its C-1' atom to the C-2 atom of the indole side chain of tryptophan (34, 35). The recognition signal for C-mannosylation is the sequence Trp-X-X-Trp and it is the first trp that becomes modified (36). The addition of mannose is enzyme catalyzed and occurs in the endoplasmatic reticulum of numerous cell lines tested (24, 37). There are currently only two reported proteins known to be C-mannosylated and they are RNase U_S(37, 38) and interleukin-12 (39).

The recognition sequence for C-mannosylation is found in the T1Rs as the familiar Trp-X-X-Trp-X-X-Trp (figure 2). We speculated that the origin our positive DIG glycan analysis and the multiple peaks resolved by MALDI-TOF MS were due in part to C-mannosylation. In collaboration with Dr. Hofsteenge, we have been able to determine that P3 and P123 do contain

C

some C-hexosylation as well as O-linked glycosylation. Confirmation that the hexose is a mannose residue will require NMR studies. As expected from the MALDI-TOF mass spectroscopy data, the glycosylation is heterogeneous, but both P123 and P3 contain some C-hexosylation on the central trp. In addition, there is O-glycosylation in the form of a disacchride on either the serine or threonine in the sequence between the first and second cysteines. The exact localization of the O-linked sugar requires further work.

5. HPLC Separation of P3 Glycoforms

Analytic high-pressure liquid chromatography (HPLC) was performed for P3 proteins expressed from both Hi5 and Sf9 cells using a C_{18} column. The column was equilibrated in 0.1% trifluoroacetic acid (TFA) and 25ug of a P3 sample in 0.1% TFA was loaded. A linear gradient of 0 to 50% acetonitrile in 0.1% TFA with a flow rate of 1ml/min was used to elute the protein. The time required for the gradient was 50 minutes and the elution was detected at 280nm. Figure 19 shows the chromatograph traces for P3 Hi5 (A) and P3 Sf9 (B). One should note that the sensitivity of the detector was higher for the P3 Hi5 sample, and hence the scale is larger. The arrow above the graph indicates the direction of the gradient, such that peak 4 was eluted first, followed by peaks three, two , and one. The primary difference between the HPLC traces for P3 Hi5 and P3 Sf9 is the relative height of peak 1. For P3 Hi5, peak 1 has the largest intensity compared to peaks 2, 3, and 4. The opposite is true for P3 Sf9, in that peak 1 has the smallest intensity compared to peaks 2, 3, and 4.

The lower portion of Figure 19 shows representative MALDI-TOF spectra for P3 Hi5 and P3 Sf9 that have not undergone HPLC separation. The internal calibrants of insulin (5734.6Da) and ubiquitin (8565.9 Da) used for mass determination are present in both of the MALDI-TOF spectra. In order to determine the origin of the four peaks resulting from the HPLC purification, I collected each of the four peaks for P3 Hi5 and P3 Sf9. I lyophilized the samples and then analyzed the products by MALDI-TOF MS, as described previously (section VI.H.2). The result showed that HPLC peak 1 contained P3 of 7250Da, which is the mass of the unglycosylated form. Therefore, HPLC peak 1 corresponded to peak 1 in the MALDI-TOF spectrum. Similar results were seen for the remaining three HPLC peaks, such that peak 2 contained protein of molecular mass equal to peak 2 in the MALDI-TOF spectrum, etc. For this reason, in Figure 19, I have labeled HPLC peaks 1, 2, 3, and 4 to correspond with the MALDI-TOF peak numbers, rather than the order in which they eluted from the C_{18} column. Interestingly, the relative size of the HPLC peak correspods to the relative intensity of the MALDI-TOF peak. We can concluded that the extent of glycosylation of P3 is dependent on the cell type used for expression and that Hi5 cells produce more unglycosylated isoforms while the Sf9 cells produce more glycosylated isoforms of P3.

24

C

6. Protease Sensitivity of P123 Monomer and Dimer

P123 was digested with increasing amounts of trypsin in 25mM Tris-Cl, 150mM Nacl, pH 8.4 at 37°C for one hour. Figure 20 shows the results of trypsin digests run on 14% SDS-PAGE under reducing (left) and (non-reducing) conditions.. The concentrations of trypsin (w/w) used were 0% (lanes 3 &10), 0.5% (lanes 4 &11), 1% (lanes 5 &12), 2% (lanes 6 &13), and 4% (lanes 7 &14). Lanes 1 and 8 contain molecular weight markers while Lanes 2 and 9 contain low molecular weight markers.

In the absence of trypsin, P123 appears as a single band of about 20kDa under reducing conditions (lane 3). Under non-reducing conditions, P123 appears as several closely spaced bands of about 20kDa, as well as one or more closely spaced bands of approximately 40kDa (lane 11). Increasing concentrations of trypsin cause P123 to be digested into two major bands and one minor band under non-reducing conditions. The larger of the two major bands runs just above the 14kDa marker, while the smaller of the two bands runs just above the 6kDa marker. The two major bands are consistent in size with two T1Rs and a single T1R module. In between the first and second T1R modules is the sequence KRFK (Figure 2) which is the likely site of trypsinization. We are in the process of sequencing the two major bands seen under non-reducing conditions. We expect the larger of the two bands to consist of P23 and the smaller to contain P1. The minor band is the same size as intact P123 and we speculate that it is derived from proteolysis of the dimeric form of P123. As discussed in section VI.A.7, we are pursuing the origin of the dimeric P123 species.

Additional information concerning the tertiary structure of P123 is obtained by examination of the digest containing 4% trypin and run with and without reduction. The non-reduced samples of this digest display two major bands, the sizes of two T1Rs and a single T1R. This would indicate that the individual T1R modules of P123 are trypsin resistant such that the disulfide bonds within a T1R maintain the integrity of the T1R unit. The reduction of this digest leads to numerous diffuse bands. This would indicate that there are solvent accessible trypsinization sites within the individual T1Rs.

7. hTSP1 Induces Apoptosis in Endothelial Cells cultured on Collagen Gels

We have utilized a two-dimensional (2D) collagen gel system to access the functional properties that TSP1 and our recombinant proteins have on microvessel endothelial cells. I have developed this method incorporating findings from the work of Scatena *et al.* (40) and Guo *et al.* (20). Scatena and collegues examined integrin involvement in endothelial cell (EC) survival upon serum withdrawal (41). These authors showed that several ECM proteins including fibronectin, collagen I, laminin, and osteopontin promote endothelial cell survival upon serum withdrawal. The authors suggest that the ligation of integrin subunits β1 and β3 mediate EC survival through

C

different pathways, since β3-induced survival, but not β1, is dependent on NF–κB. I required the use of serum-free conditions when examining the effect of TSP1 on endothelial cells since TSP1 is found in serum at approximately 25-30ug/ml. Guo and collegues reported the ability of TSP1 to induce apoptosis in EC under defined conditions (20). These authors showed that TSP1 and peptides to portions of the type 1 repeats induce apoptosis in endothelial cells when the cells were seeded in media containing 5% serum on uncoated surfaces. The authors also show that coating the surface with fibronectin (FN) reduced the effect of TSP1 and the peptides. One conclusion is that TSP1 sends a signal to ECs to undergo apoptosis in the absence of a strong survival signal, such is as provided by a FN matrix. Since FN can utilize the β1 and β3 integrins and in consideration of the work of Scatena discussed above, one might hypothesize that TSP1 is not able to over-ride the signals coming from β1, β3, or a combination of β1 and β3 ligation. My studies have extended the understanding of TSP1 induced apoptosis of ECs. This is practically important due to the recognition that one mechanism of action for angiogenesis inhibitors is by induction of apoptosis in ECs (42).

Type I collagen gels were poured in 24-well tissue culture plates and allowed to polmerize for 2 hours at 37°C. The final concentration of collagen was 0.5mg/ml. Endothelial cells were seeded on the gels at sub-confluent density in media containing 0.5% serum. The cells were allowed to spread overnight. The next day the gels were washed with serum-free media. The collagen gels, unlike a collagen coated surface, allow the ECs to organize into interconnecting monolayer-like patches which possess a cobblestone morphology. Consistent with the work of Scatena et al.(40), we found that ECs on collagen gels survive under serum-free conditions for up to 9 days. The addition of TSP1 (10ug/ml) to the media resulted in distinct morphologic changes to the ECs followed by cell death (Figure 21). The effect was dose dependent such that increasing concentrations of TSP1 caused increased cell death (Figure 22). In addition, the effect of TSP1 was diminished when increasing concentrations of serum was added to the media and no effect of exogenous TSP1 was observed in media containing 10% serum. We can hypothesize that under serum free conditions, TSP1 is able to over-ride the survival signal provided by ligation of the β1 integrin to the collagen gel. Additionally, factors present in the serum are able to contribute to the survial signals provided by the collagen gel and together surpass the death signal sent by TSP1. Since the β1 and β3 integrins send survival signals for ECs through distinct mechanisms, our lab plans to investigate the effect of TSP1 on ECs seeded on fibrin gels which would involve ligation of the β3 integrin. As discussed in the work of Scatena et al (40), the mechanism of β1–induced EC survival is not known; however, investigation in this area would be of interest to our lab due in part to our extensive work with β1 transfected cells.

Consistent with the work of Guo et al (20), I have found that the increased death caused by TSP1 is due to apoptosis. Using a modified Wright stain, I have been able to visualize nuclear

26

C

fragmentation in ECs seeded on collagen gels following 42 hours of treatment with 10ug/ml TSP1 under serum free conditions (Figure 23). In addition, I have found that the effect of TSP1 on ECs seeded on collagen gels is more extensive than when the cells are seeded on collagen coated surfaces. This is consistent to the work of Guo *et al* (20), in which the authors induction of apoptosis by TSP1 in EC seeded either on uncoated surfaces or FN coated surfaces was weak. Since nuclear fragmentation is only one hallmark of apoptotic cells, we will examine the ability of the cells treated in this manner to stain positive for annexin and to display DNA fragmentation in order to confirm that TSP1 is causing apoptosis.

In addition, we are examining which domains of TSP1 are responsible for the apoptotic effect. We have expressed overlapping segments of hTSP1 and 2 using the COCO expression system, as shown in Figure 24. Using the 2D collagen gels system, I have tested recombinant proteins that span the entire TSP1 molecule. In general, I have found that 10-40nM TSP1 is the best range to examine the effect on ECs. Since TSP1 is a trimer, I have used concentrations for the recombinant proteins of 30-120nM. I found that no recombinant protein had the same effect on EC morphology and death as intact TSP1. It is likely that the effect of intact TSP1 arises from at least two distinct portions of the intact TSP1. However, we plan to determine the active sites responsible for TSP1 induced EC apoptosis.

8. The Effect on Endothelial Cell Morphology by P3 and P123

In addition to using the 2D collagen gel system to access the morphologic and apoptotic effect of hTSP1 on ECs, I have used it to examine the effect of several of our recombinant proteins, including P3 and P123. The ECs were seeded on collagen gels as described previously. The cells were treated with serum-free media supplemented with 10ug/ml of the recombinant protein. The cells were fed and fresh protein was added every 2-3 days. The recombinant proteins used were P3, the third T1R; P123, the first through the third T1R; and E3Ca1, the third EGF-like repeat through the C-terminus of TSP1. The results are shown in Figure 25 and the findings are discussed below .

The control ECs remain organized on the collagen gel as interconnecting monolayer patches. Treatment of the EC with 10ug/ml E3Ca1 in serum-free media caused the ECs to decrease the size of their monolayer patches, to elongate, and to die. Therefore, a portion of the death induced by TSP1 can be attributed to the C-terminal portion of the molecule. This finding is of particular interest since our lab has more precisley mapped many of the antibodies to TSP1, including A4.1, by utilizing our overlapping recombinant TSP1 constructs (Manuscript in preparation; Figure 24). The monoclonal-antibody A4.1 is known to block the angiogostatic activity of TSP1 and it was previously thought to map to the T1Rs. We have now been able to show that A4.1 binds the third EGF-like repeat in TSP1. The mapping of A4.1 to the third EGF-like repeat is consistent with our finding of increased EC death induced by a recombinant protein (E3Ca1) containing this region. This

C

finding is also consistent with some of the original work done by Bouck and collegues (2) in which they found the 50/70kDa trimer inhibited neovascularization in rat corneas, and inhibited EC migration in response to bFGF. The 50/70 kDa fragment is believed to span the oligomerization, procollagen, T1R, and T2R modules. Therefore, the proteolytic 50/70kDa anti-angiogenic fragment of TSP1 and E3Ca1 contains the region (E3) to which A4.1 maps.

Treatment of the ECs with 10ug/ml P123 or P3 caused monolayer areas to enlarge and ECs within these monolayers to be more tightly packed. There was approxiamtely a 30% increase in the number of nuclei per unit area within a confluent monolayer patch when compared to control EC. The same trend occurred when I used as little as 30nM of either P3 and P123. Based on the morphology changes, we will examine if the T1Rs cause the ECs to proliferate, migrate together, or alter expression of cell-cell junctional proteins such as vascular endothelial (VE) cadherin.

My data concerning the activity of the T1Rs on ECs contrasts with the data reported by Guo *et al.* (20), in which small T1R-derived peptides containing D-amino acids (retro-inverso) induce apoptosis in ECs. Based on the work of Bouck *et al* (19) (described in Section VI.B.2), these peptides derive their activity from the presence of the D-amino acids and this activity could involve a mechanism that is different from that of TSP1. However, the D-amino acid peptides are promising therapeutic anti-angiogenic molecules. It will be interesting to compare the activity of the native T1Rs to T1R proteins that we have denatured through various methods. Given that we have recombinantly expressed, biophysically characterized, and shown the T1Rs to be in the native state, we our uniquely qualified to determine the activity of this region of TSP1.

One reason to pursue the potential link between VE-cadherin, the T1R recombinant proteins, and TSP1 stems from a recent publication by Carmeliet *et al.* (43). The authors found that altered VE-cadherin gene expression impaired remodeling and maturation of the vasculature. Deficiency or truncation of VE-cadherin induced EC apoptosis and abolished transmission of EC survival signals by VEGF-A. We speculate, as do the authors, the role of VE-cadherin expression in vascular maintenance and angiogenesis in the adult. The authors point to a role due to the expression of VE-cadherin in the adult vasculature and due to the ability of a VE-cadherin antibody to induces EC apoptosis in adult mice. Using the 2-Dimensional gel system, we are suited to examine the effect TSP1 and recombinant TSP1 fragments have on VE-cadherin expression and EC survival.

9. The effect of hTSP1 recombinant fragments of TSP1 on Endothelial Cell Migration

Endothelial cell migration is one of the steps in angiogenesis. An *in vitro* assay using a modified Boyden chamber allows quantitation of EC migration in response to a stimulant. The assay also allows potential inhibitors to be included for determination of their anti-migratory activity. This assay has been used extensively in the thrombospondin literature. At low

C

concentrations TSP1 inhibits EC migration in response to various stimulants including bFGF and VEGF.

We have used this assay to test the effect of TSP1 and two recombinant fragments of TSP1 on EC migration in response to a lipid mediator. Dr Tracee Panetti has found that sphingosine-1-phosphate (S1P) is a potent inducer of EC migration (manuscript submitted). S1P acts through the G-protein coupled receptors of the Edg family which is different from the receptors utilized by bFGF and VEGF. Therefore, the effect of TSP1 on EC migration induced by S1P is unknown.

Microvessel ECs were starved of growth factor overnight. Cells were seeded using serum-free media in the bottom wells of a 48-well chemotaxis chamber at 1.4×10^4 cells/well. The chamber was assembled with a collagen I coated 5uM pore filter. The chamber was inverted at 37°C for 2 hours to allow the cells to attach. S1P, at 1uM in DMEM/0.2% fatty acid free BSA, was added to the top wells with or without TSP1 or recombinant proteins. The chamber was returned to 37°C and the cells allowed to migrate for 4 hours. The chamber was disassembled, the filter was scraped to remove unmigrated cells, and the filter was fixed and stained with DiffQuik. Eight fields were counted per well and summed. All samples were done in triplicate. Data from one representative experiment is presented in Figure 26. The number of cells migrated is shown as a percent of the total number of cells that migrated in response to S1P alone. All concentrations of TSP1 tested inhibited migration with the lowest (2.5nM) and highest (40nM) concentrations having the maximal effect. The recombinant protein delNo1 is a monomer and consists of the procollagen domain through the C-terminus of TSP1. It is analogous to the GP140 fragment of hamster TSP1 initially found to have anti-angiogenic activity(1). All concentrations of delNo1 tested inhibited migration to a similar level as TSP1, with the exclusion of the lowest and highest TSP1 concentrations. The recombinant protein NoC1 is trimeric and contains the N-terminus through the procollagen module of hTSP1. NoC1 had a striking effect on EC migration. It enhanced migration in response to 1uM S1P in a dose dependent manner. One explanation for this increase in endothelial cell migration comes from the effect of TSP1 on focal adhesions. The N-terminal heparin binding domain of TSP1 is known to stimulate a rapid loss of focal adhesions in ECs and cytoskeletal reorganization, with the effect complete within 20 minutes (44, 45, 46). Focal adhesion loss is consistent with a pro-migratory state. We can speculate that NoC1's activity in the migration assay is due to its ability to stimulate focal adhesion dissasembly in ECs. Our lab plans to continue investigation into how the different modules of TSP1 affect EC migration.

29

C

VII. Key Research Accomplishments

A. Expression of P3 and P123

1. The use of the pCOCO expression system allowed P3 and P123 to be readily purified from conditioned media of baculovirally infected High 5 cells in the absence of denaturants.
2. The expression of P123 was >10mg/L while that of P3 was 1-2mg/L.
3. The proteins were pure as determined by SDS-PAGE and MALDI-TOF MS.
4. The N-Terminus of both P3 and P123 are homogeneous and the GP67 signal sequence was cleaved at the anticipated site.

B. Determination of Mass and Disulfide Bond Content of P3 and P123

1. Using MALDI-TOF MS, four masses were determined for P3 and the mass of the first peak agrees with the expected mass based on knowledge of the N-terminus and the cDNA.
2. At least two masses were associated with P123, with the mass of the first peak close to the expected mass.
3. The mass difference between the peaks for P3 and P123 was in the range 154-176Da.
4. P3 contains three disulfide bonds, the expected number, and there are no free thiols.

C. Glycosylation Analysis of P3 and P123

1. The DIG Glycan Detection system has shown both P3 andP123 to be glycosylated.
2. The multiple masses determined for P3 and P123 by MALDI-TOF MS represent different glycoforms of the protein.
3. The heterogeneous glycosylation results from O-linked and C-linked sugars.
4. The C-linked glycosylation is on the central trp in the sequence W-X-X-W-X-X-W.
5. The cell type used for expression determines the extent of glycosylation, such that Hi5 cells produce less glycosylated recombinant protein than Sf9 cells.
6. The different glycoforms of P3 can be isolated by HPLC.

D. Examination of the Environment of the conserved Tryptophans in the P3 and P123

1. In the native state, both P3 and P123, are in a slightly polar/non-polar environment based on the fluorescence wavelength of maximum emission (λ_{max}).
2. In the native state, the trps are in close contact with residues that cause the fluorescence signal to be quenched. These quenching residues are displaced from the

C

immediate environment of the trps by disulfide bond reduction, chemical denaturation, or heat-induced denaturation.

3. Disulfide bond reduction causes a rapid change in the polarity of the trp environment but a slower change in the movement of quenching residues away from the trps.

4. In the native state, the trps are accessible to small molecules at least the size of glycerol, which has a mean diameter of 5.2Å. Thus, the trps are solvent accessible.

5. The trps in P3 and P123 are in an ordered/chiral structure.

6. There is no difference in the chirality of the trps at 25°C or 37°C. However, the chirality of the trps is lost by 55°C.

7. There is an overall difference in the chirality of the 9 trps in the three tandem T1Rs of P123 compared to the three trps in the single T1R of P3.

E. Structural properties of P3 and P123

1. The recombinant T1Rs expressed, P3 and P123, contain secondary structure very similar to the non-recombinant protein properdin, which contains six T1Rs in series.

2. Heating P3 or P123 causes a transition to a random coil conformation. The T_m for denaturation for P3 and P123 is 55°C.

3. The secondary structure of P3 and P123, as determined by Far-UV CD at 25°C, are very similar. There are no apparent changes induced by expressing the modules in series. Each modules is an independent folding unit.

4. There is no difference in the secondary of structure for either P3 or P123 when the temperature is raised from 25°C to 37°C (physiologic temperature).

5. P123 contains a trypsin senstive site located between the first and second T1Rs.

6. The integrity of the individual T1Rs are maintained by the disulfides bonds in the presence of trypsin. There are solvent accessible trypsin sites present in the native individual T1Rs.

7. The disulfide bonds contribute to the thermal stability of the T1Rs, since reduction causes the transition to a random coil to occur at a lower temperature. However, the transition to a random coil induced by disulfide bond reduction is slow at 25°C.

F. Effect of hTSP1 and recombinant TSP1 fragments on Endothelial Cells

1. TSP1 decreases survival of ECs on collagen I gels in a dose dependent manner .

2. The effect of TSP1 on EC survival is inhibited by factors present in serum.

3. TSP1 decreases EC survival by inducing programmed cell death, or apoptosis.

4. P3 and P123 do not decrease survival of ECs on a collagen I gel.

C

5. Treatment of ECs on collagen I gels with as little as 30nM P3 or P123 causes an increase in the number of EC per unit area. P3 and P123 may act as positive regulators of EC survival.

VIII. Reportable Outcomes

A. Publications
  1. Abstracts presented:
     a. The 12th Symposium of the Protein Society July 25-29, 1998
        Expression of Characterization of Human Thrombospondin 1 Type 1 Repeats
        Krisitn G. Huwiler, Douglas S. Annis, Deane F. Mosher

     b. Genetics, Genomics, and Molecules Symposium May 23-25, 1999
        Expression of human Thrombospondin 1and 2 Modules:
        Biophysical and Immunological Characterization
        Kristin G. Huwiler, Tina Misenheimer, Douglas Annis, Deane Mosher

  2. Manuscripts in preparation:
     a. Biophysical Characterization of the Baculovirally Expressed Third Type 1 Repeat of human Thrombospondin-1
     b. Structural and Functional Comparison of two recombinant proteins derived from human Thrombospondin-1: the Third Type 1 Repeat (P3) and the First, Second, and Third Type 1 repeats in tandem (P123)
     c. The Modules of human Thrombospondin I responsible for its Apoptotic effect on Endothelial Cells

B. Patents and Licenses Applied for: None

C. Degree Obtained
   Ph.D., Biophysics, University of Wisconsin-Madison Fall 1999

D. Development of Cell Lines, Tissue or Serum Repositories: None

E. Databases ans Animal Models Developed: None

C

G. Employment Opportunities Applied for: To be utilized after completing degree

IX. Conclusions

The purpose of this work was to recombinantly express, purify, and biophysically characterize the T1Rs of human TSP1. I have successfully expressed and purified the T1R modules in the native state. The environment of the conserved tryptophans, the glycosylation of the modules, the thermal stability as well as the role of the disulfides in stability has been established. In addition, I have begun characterization of the role of the native T1Rs on endothelial cells and the activity of TSP1 on endothelial cell apoptosis. This work serves as a starting point for understanding the function of the T1R and the primary, secondary, and/or tertiary structure necessary for its activity.

The implications of the research I have conducted extend into the use of angiostatic molecules to inhibit tumor induced blood vessel growth. The initial growth of a human tumor usually does not require a direct blood vessel supply. However, in its absence, a solid tumor is limited in size to a 1-2 mm diameter and the metastatic potential of the tumor is thwarted (6, 7). The switching of cells within the tumor to an angiogenic phenotype stimulates new blood vessel growth toward the tumor and is dependent on the balance between stimulators and inhibitors of angiogenesis in the ECM (8). In the past year and a half, much attention has been focused on the angiostatic proteins angiostatin (9, 10) and endostatin (11, 12) which have been shown in animal studies to shrink primary tumors and decrease metastases without signs of resistance. These proteins, like TSP1, hold great promise in clinical use both alone and in combination with traditional chemotherapies to shrink primary tumor masses, prevent micro-metastases from expanding, and thereby indefinitely prolong the time a patient remains free of detectable cancer. However, the use of intact TSP1 clinically is prohibitive due to its large size (450kDa). Smaller molecules are better suited for use as drugs since they are less expensive to manufacture and the systemic bioactivity of these molecules is longer. The individual modules of TSP1 would be more amenable for use as drugs. Therefore, the determination of the activity of the native modules of TSP1 is a critical step if the angiostatic activity of TSP1 is to be used clinically. The work I have conducted helped define the biophysical properties and the activity of one of modules in TSP1.

C

X. References

1. D. J. Good, et al., *Proceedings of the National Academy of Sciences of the United States of America* **87**, 6624-8 (1990).

2. S. S. Tolsma, et al., *Journal of Cell Biology* **122**, 497-511 (1993).

3. P. Bagavandoss, J. W. Wilks, *Biochemical & Biophysical Research Communications* **170**, 867-72 (1990).

4. S. S. Tolsma, M. S. Stack, N. Bouck, *Microvascular Research* **54**, 13-26 (1997).

5. O. V. Volpert, J. Lawler, N. P. Bouck, *Proceedings of the National Academy of Sciences of the United States of America* **95**, 6343-8 (1998).

6. J. Folkman, R. Cotran, *International Review of Experimental Pathology* **16**, 207-48 (1976).

7. J. Folkman, *Cancer Research* **34**, 2109-13 (1974).

8. J. Folkman, *Nature Medicine* **1**, 27-31 (1995).

9. M. S. O'Reilly, et al., *Cell* **79**, 315-28 (1994).

10. M. S. O'Reilly, L. Holmgren, C. Chen, J. Folkman, *Nature Medicine* **2**, 689-92 (1996).

11. T. Boehm, J. Folkman, T. Browder, M. S. O'Reilly, *Nature* **390**, 404-7 (1997).

12. M. S. O'Reilly, et al., *Cell* **88**, 277-85 (1997).

13. T. S. Panetti, B. J. Kudryk, D. F. Mosher, *Journal of Biological Chemistry* **274**, 430-7 (1999).

14. J. Sottile, J. Schwarzbauer, J. Selegue, D. F. Mosher, *Journal of Biological Chemistry* **266**, 12840-3 (1991).

15. F. Zhang, D. J. Robbins, M. H. Cobb, E. J. Goldsmith, *Journal of Molecular Biology* **233**, 550-2 (1993).

16. K. F. Nolan, K. B. Reid, *Methods in Enzymology* **223**, 35-46 (1993).

17. T. C. Farries, J. P. Atkinson, *Journal of Immunology* **142**, 842-7 (1989).

18. K. B. Reid, J. Gagnon, *Molecular Immunology* **18**, 949-59 (1981).

19. D. W. Dawson, et al., *Molecular Pharmacology* **55**, 332-338 (1999).

20. N. Guo, H. C. Krutzsch, J. K. Inman, D. D. Roberts, *Cancer Research* **57**, 1735-42 (1997).

21. C. A. Smith, M. K. Pangburn, C. W. Vogel, H. J. Muller-Eberhard, *Journal of Biological Chemistry* **259**, 4582-8 (1984).

22. R. W. Woody, *European Biophysics Journal* **23**, 253-62 (1994).

23. D. Freifelder, . (W.H. Freeman and Company, New York, 1982) pp. 494-536.

24. M. A. Doucey, D. Hess, R. Cacan, J. Hofsteenge, *Molecular Biology of the Cell* **9**, 291-300 (1998).

25. A. A. Kossiakoff, et al., *Protein Science* **3**, 1697-705 (1994).

26. W. Somers, M. Ultsch, A. M. De Vos, A. A. Kossiakoff, *Nature* **372**, 478-81 (1994).

27. O. Livnah, et al., *Science* **273**, 464-71 (1996).

34

28. A. M. de Vos, M. Ultsch, A. A. Kossiakoff, *Science* **255**, 306-12 (1992).

29. J. Lawler, J. E. Connolly, P. Ferro, L. H. Derick, *Annals of the New York Academy of Sciences* **485**, 273-87 (1986).

30. D. D. Roberts, *Cancer Research* **48**, 6785-93 (1988).

31. N. H. Guo, et al., *Proceedings of the National Academy of Sciences of the United States of America* **89**, 3040-4 (1992).

32. N. H. Guo, H. C. Krutzsch, E. Negre, V. S. Zabrenetzky, D. D. Roberts, *Journal of Biological Chemistry* **267**, 19349-55 (1992).

33. J. Takagi, T. Fujisawa, T. Usui, T. Aoyama, Y. Saito, *Journal of Biological Chemistry* **268**, 15544-9 (1993).

34. J. Hofsteenge, et al., *Biochemistry* **33**, 13524-30 (1994).

35. T. de Beer, J. F. Vliegenthart, A. Loffler, J. Hofsteenge, *Biochemistry* **34**, 11785-9 (1995).

36. J. Krieg, et al., *Molecular Biology of the Cell* **9**, 301-9 (1998).

37. J. Krieg, et al., *Journal of Biological Chemistry* **272**, 26687-92 (1997).

38. A. Loffler, et al., *Biochemistry* **35**, 12005-14 (1996).

39. O. Livnah, et al., *Science* **283**, 987-90 (1999).

40. P. Kannus, et al., *Histochemical Journal* **30**, 799-810 (1998).

41. M. Scatena, et al., *Journal of Cell Biology* **141**, 1083-93 (1998).

42. S. Stromblad, J. C. Becker, M. Yebra, P. C. Brooks, D. A. Cheresh, *Journal of Clinical Investigation* **98**, 426-33 (1996).

43. P. Carmeliet, et al., *Cell* **98**, 147-157 (1999).

44. J. E. Murphy-Ullrich, M. Hook, *Journal of Cell Biology* **109**, 1309-19 (1989).

45. J. A. Greenwood, M. A. Pallero, A. B. Theibert, J. E. Murphy-Ullrich, *Journal of Biological Chemistry* **273**, 1755-63 (1998).

46. J. E. Murphy-Ullrich, S. Gurusiddappa, W. A. Frazier, M. Hook, *Journal of Biological Chemistry* **268**, 26784-9 (1993).

XI. Appendices

U.S. Army Medical Research and Materiel Command
Attn: MCMR-RMI-S
504 Scott Street
Fort Detrick, Maryland   21702-5012

Dear Sir or Madame,

I am writing to request that all of the material in the **Body, Key Research Accomplishments,** and the **Data Figures** found in the **Appendices** be protected from broad distribution at this time since the work is unpublished. I am currently in the process of preparing two of the manuscripts I have listed in the **Reportable Outcomes** section. However, I would appreciate my data, including methodology and details of the construction of the baculoviral transfer vector pCOCO, remain confidential until the work is published. All pages to be considered confidential are marked with the letter C in the lower right corner of the page. Thank you for your time and cooperation.

Sincerely,

Kristin G. Huwiler

Figure 1: Trimeric Organization of TSP1
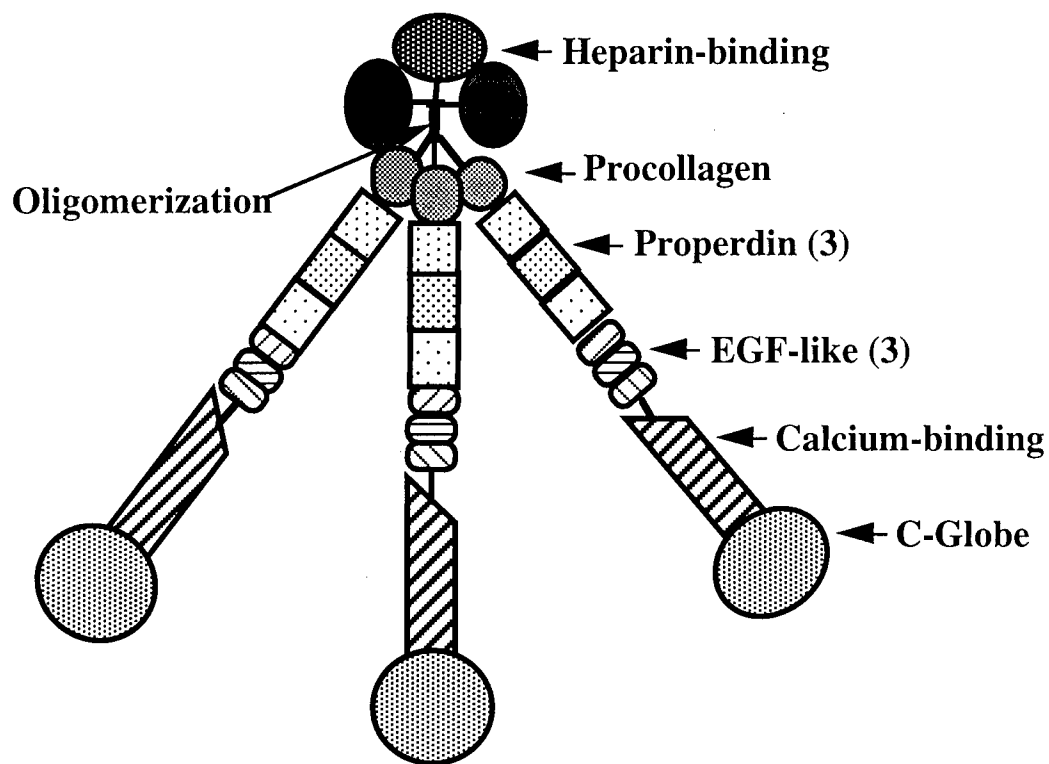
Figure 2: Amino Acid Sequence of hTSP1 Type 1 Repeats

```
                       1       2           3           4         5     6
1st SDSADDGWSPWSEWTSCSTSCGNGIQQRGRSCDSLNNR.....CEGSSVQTRTCHIQECDKRF
2nd    KQDGGWSHWSPWSSCSVTCGDGVITRIRLCNSPSPQMNGKPCEGEARETKACKKDACP
3rd     INGGWGPWSPWDICSVTCGGGVQKRSRLCNNPAPQFGGKDCVGDVTENQICNKQDCPI
```

C

Figure 3: Features of Baculovirus Transfer Vector pCOCO

	Thrombin Site										**Histidine-Tag**						
Protein	L	E	L	V	P	R	G	S	A	A	G	H	H	H	H	H	H	Z
DNA	t cta gaa	tta	gtg	cct	cgc	gga	agc	gct gca ggg	cat	cac	cat	cac	cat	cac	tag gac cta ct

| **XbaI** | | | | **PstI** | | | | **PpumI** |

NdeI 9557

AmpR

ColE ori

pAcGP67.COCO

9772 base pairs

Polyhedrin Promoter

gp67 Secretion Signal

Baculovirus Sequence

3770 NaeI

COCO

MCS 4251 BamHI
      4255 SmaI
      4255 XmaI
      4266 XbaI

38

C
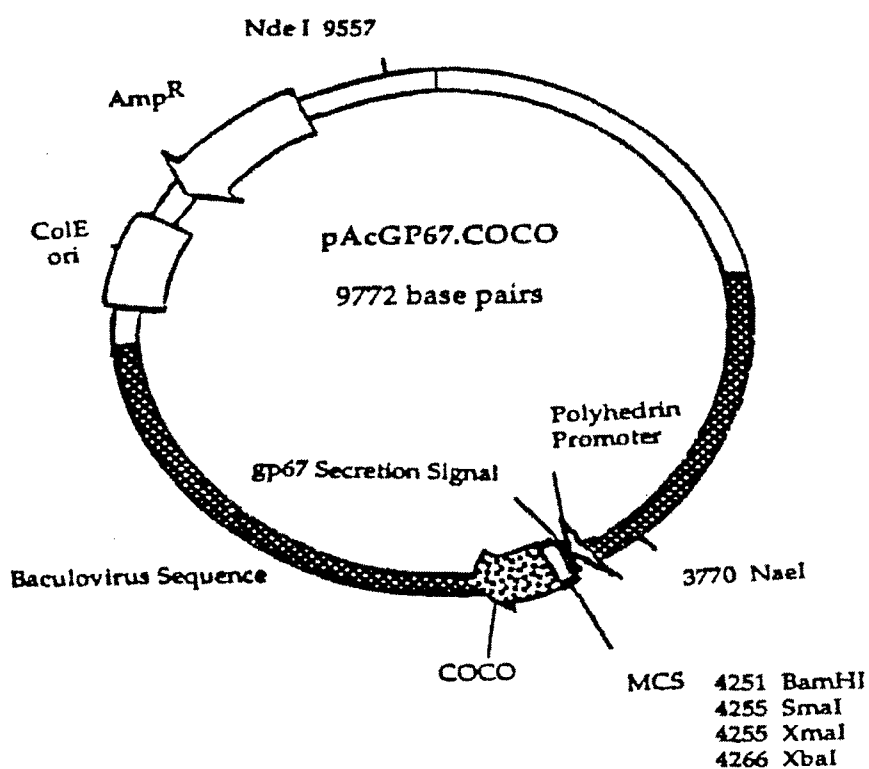
Figure 4

A. Primers used to Construct pCOCO

COCO Forward   **5'** ctt cta gaa tta gtg cct cgc gga agc gct gca ggg cat cac c   **3'**

COCO Reverse   **5'** ag tag gtc cta gtg atg gtg atg gtg atg ccc tgc agc gct tcc   **3'**

B. Primers used to Amplify hTSP1 Type 1 Repeats

P123 Forward   **5'** tcc ccc ggg agc gac tct gcg gac gat gg   **3'**

P123 Reverse   **5'** ggg tct aga att gga cag tcc tgc ttg ttg c   **3'**

P3 Forward   **5'** tat ccc ggg atc aat gga ggc tgg ggt cct tgg   **3'**

Figure 5: Fusion Proteins Expressed using pCOCO

			Thrombin Site| His-Tag	Size (kDa)
General	ADPG	(------------------INSERT----------------)	LE<u>LVPRGS</u>AAG<u>HHHHHH</u>	
P123.COCO	ADPG		LE<u>LVPRGS</u>AAG<u>HHHHHH</u>	21.1
P3.COCO		ADPG	LE<u>LVPRGS</u>AAG<u>HHHHHH</u>	8.4
Post-Thrombin Cleavage				
P123.C	ADPG		LE<u>LVPR</u>	20.0
P3.C		ADPG	LE<u>LVPR</u>	7.3

C

Figure 6: Elution Profile of P123.COCO from the Nickel Column

C
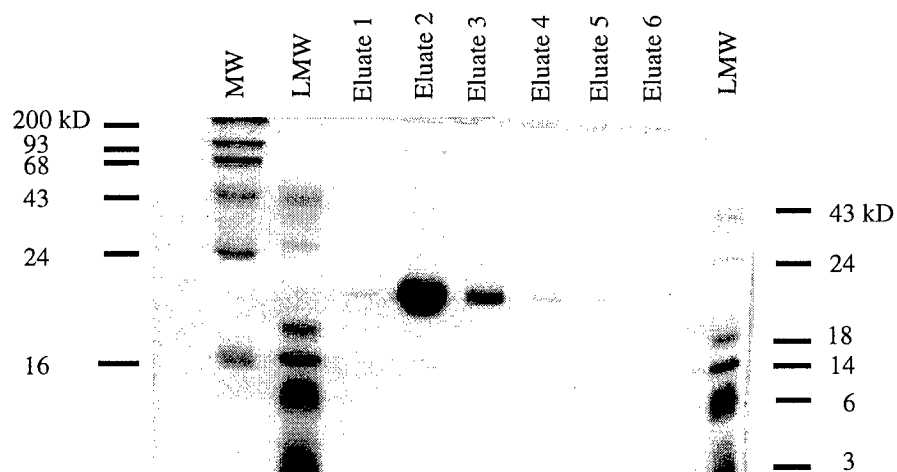
Figure 7: 12-20% SDS-PAGE of P123 and P3

MWM   LMWM   P123   P3

Non-Reduced

MWM   LMWM   P123   P3

Reduced

C
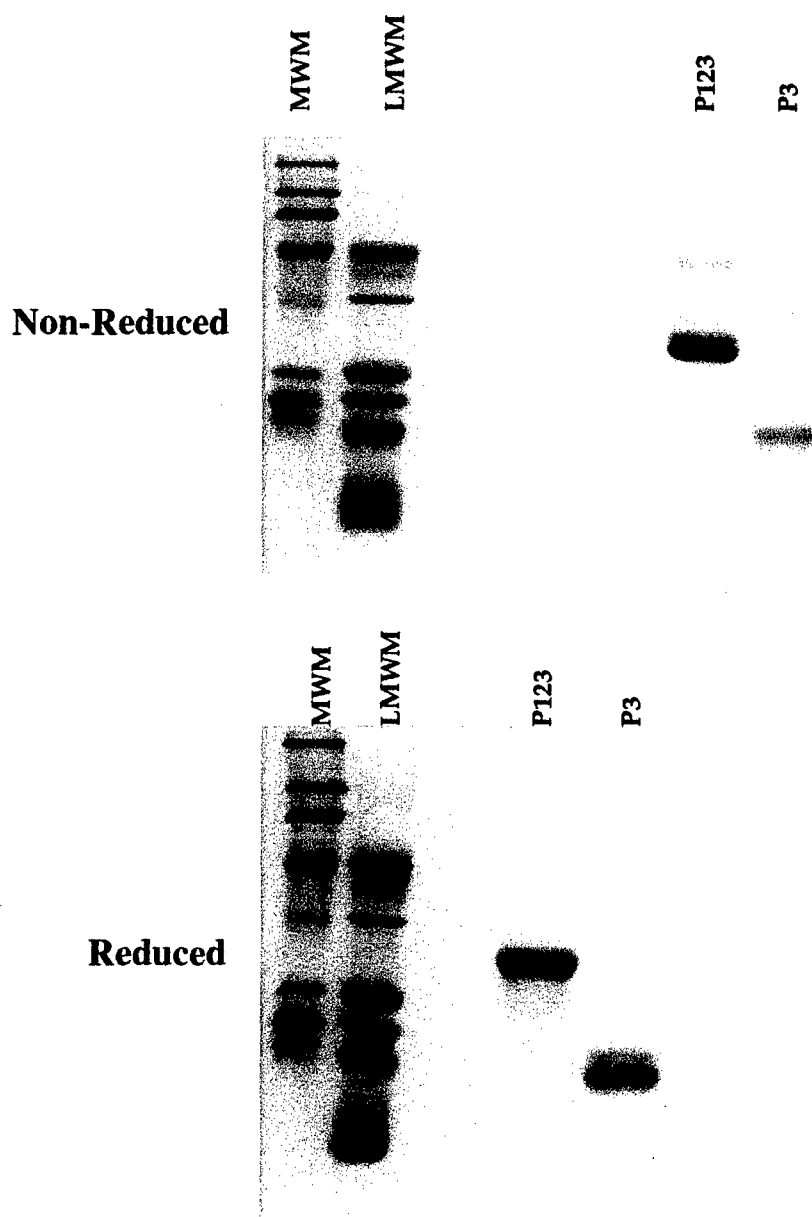
Figure 8: Elution Profile of P3.COCO

C
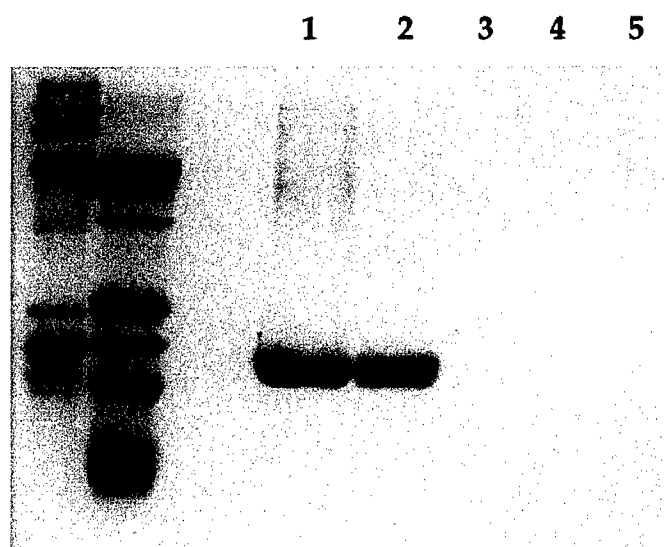
Figure 9: N-Terminal Sequence Determination

A. Amino Acid Sequences of Constructs

1. P123.COCO

```
            |------------Proposed GP67 signal sequence------------|
   1    MLLVNQSHQGFNKEHTSKMVSAIVLYVLLAAAAHSAFAADPGSDSADDGW
  51    SPWSEWTSCSTSCGNGIQQRGRSCDSLNNRCEGSSVQTRTCHIQECDKRF
 101    KQDGGWSHWSPWSSCSVTCGDGVITRIRLCNSPSPQMNGKPCEGEARETK
 151    ACKKDACPINGGWGPWSPWDICSVTCGGGVQKRSRLCNNPTPQFGGKDCV
 201    GDVTENQICNKQDCPILELVPRGSAAGHHHHHH
```

2. P3.COCO

```
            |-------------Proposed GP67 signal sequence-----------|
   1    MLLVNQSHQGFNKEHTSKMVSAIVLYVLLAAAAHSAFAADPGINGGWGPW
  51    SPWDICSVTCGGGVQKRSRLCNNPTPQFGGKDCVGDVTENQICNKQDCPI
 101    LELVPRGSAAGHHHHHH
```

B. Results of N-Terminal Sequence Analysis

Cycle	Sequenced from P123	Match	Sequenced from P3	Match
1	A	+++	A	+++
2	D	+++	D	+++
3	P	+++	P	+++
4	G	+++	G	+++
5	S	+++	I	+++
6	D	+++	N	+++
7	S	+++	G	+++
8	A	+++	G	+++
9	D	+++		
10	D	+++	P	+++

C

Figure 10: UV Wavelength Scans of Recombinant T1Rs of hTSP1
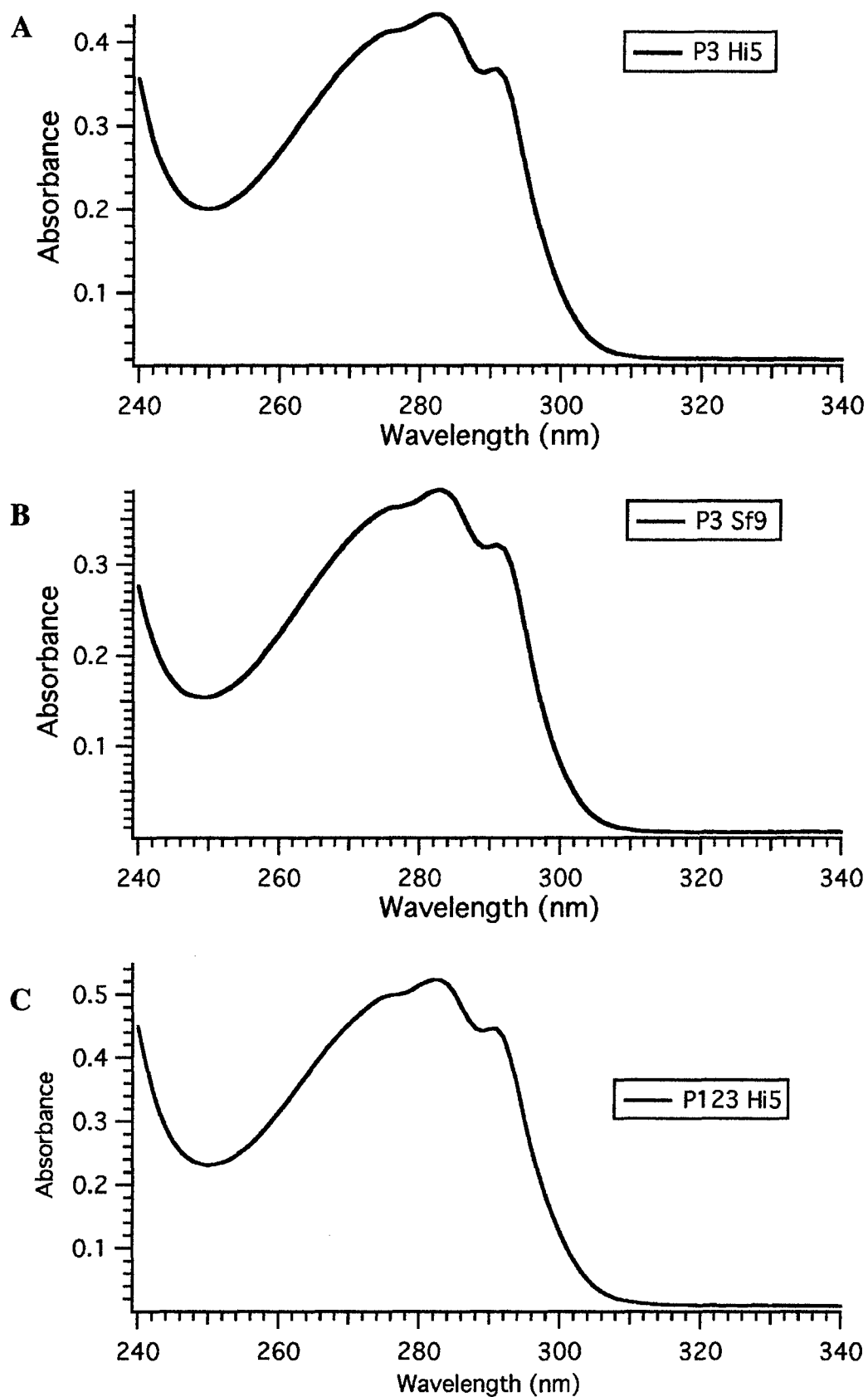
Figure 11: Far-UV Circular Dichroism of P3 and P123

A.

Legend:
- P3, 25°C
- P3, 37°C
- P3, 45°C
- P3, 50°C
- P3, 55°C
- P3, 60°C
- P3, 65°C

y-axis: $[\Theta]_{MRW} \times 10^{-3}$ (deg cm^2/decimol)
x-axis: Wavelength (nm)

B.

Legend:
- P123, 25°C
- P123, 37°C
- P123, 45°C
- P123, 50°C
- P123, 55°C
- P123, 60°C
- P123, 65°C

y-axis: $[\Theta]_{MRW} \times 10^{-3}$ (deg cm^2/decimol)
x-axis: Wavelength (nm)

C.

Legend:
- P3, 25°C
- P123, 25°C

y-axis: $[\Theta]_{MRW}$ (deg cm^2/decimol)
x-axis: Wavelength (nm)

C
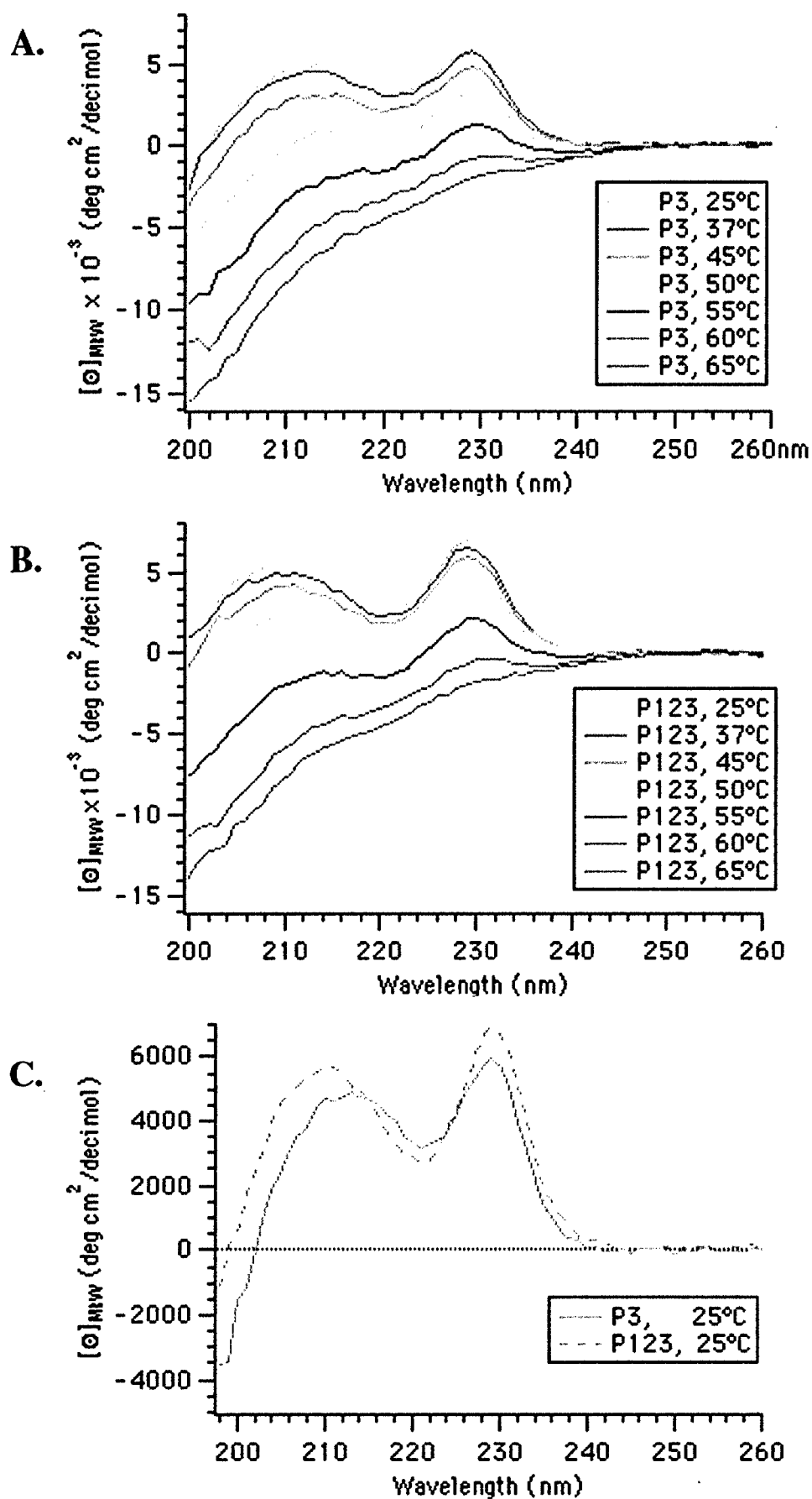
Figure 12: Near-UV Circular Dichroism of P3 and P123

A.

B.

C.

C
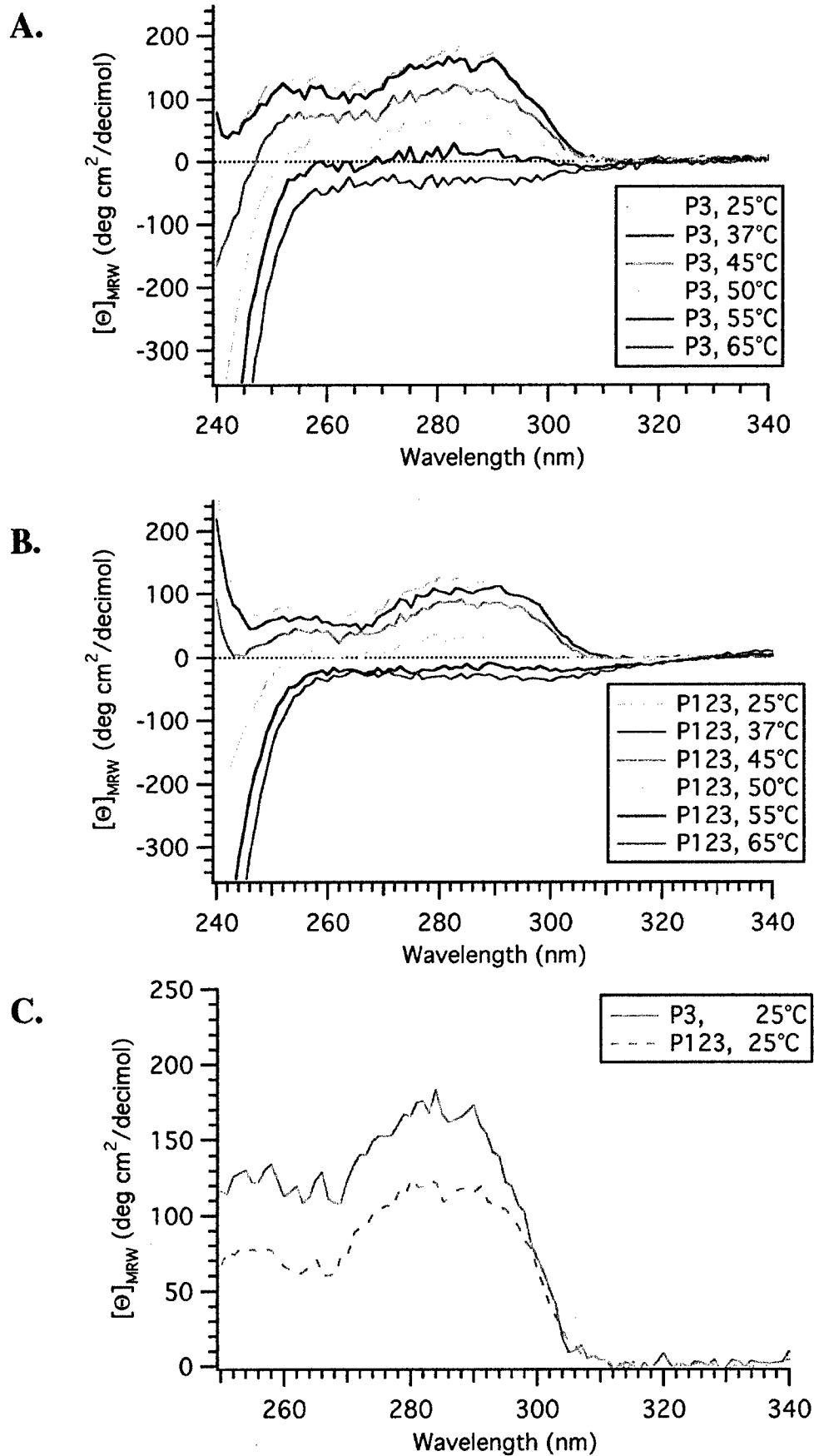
Figure 13: Effect of DTT on P3 Monitored by Far-UV CD

C
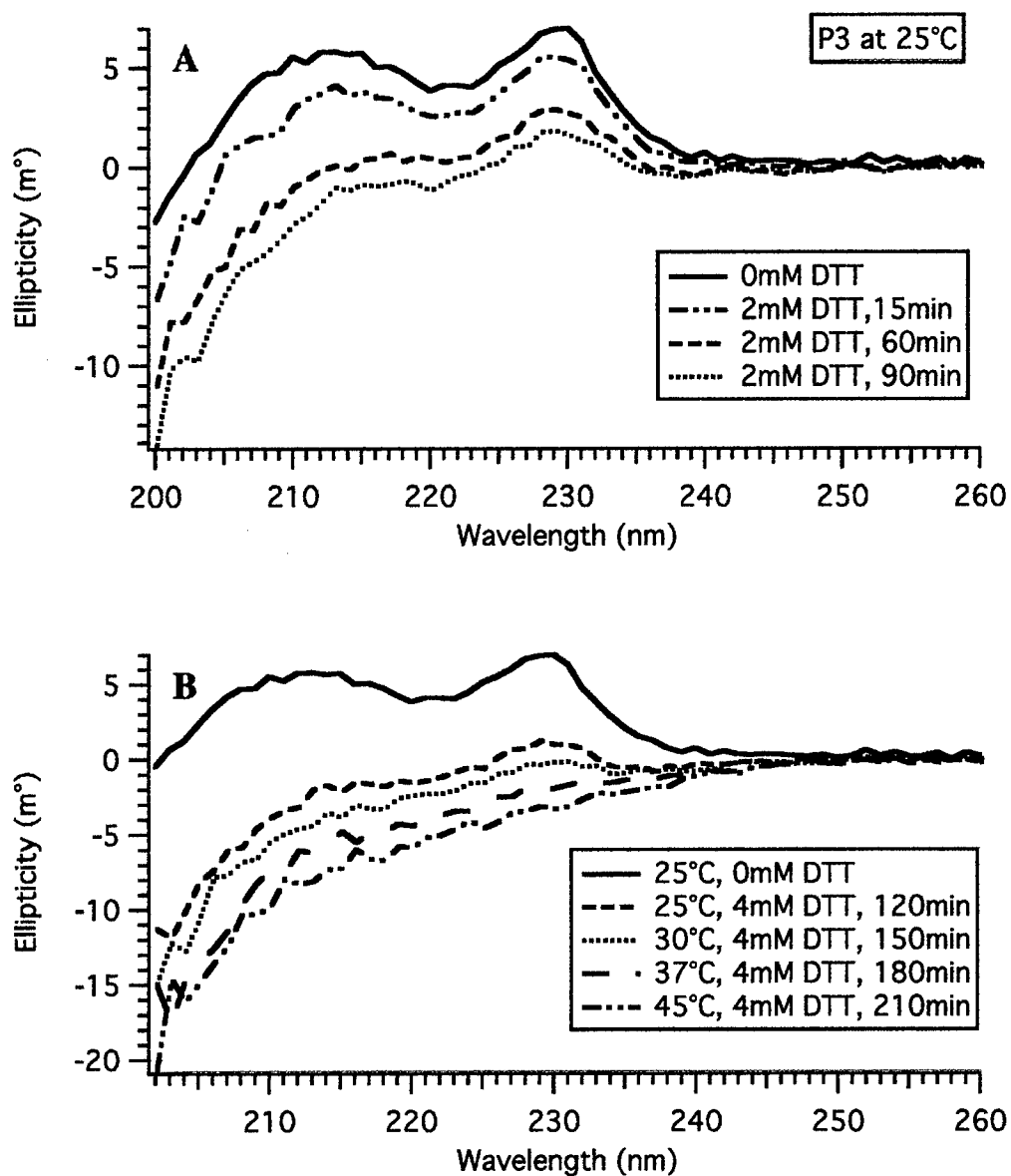
Figure 14: Dual Monitoring of CD and Fluorescence
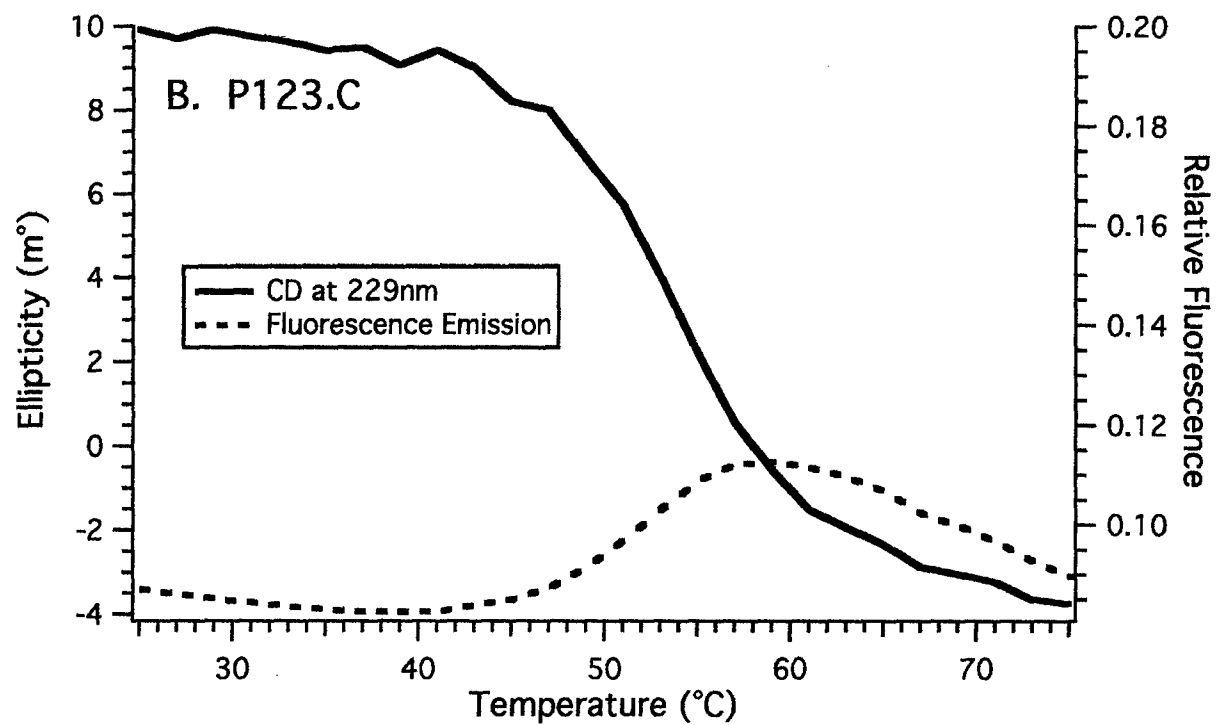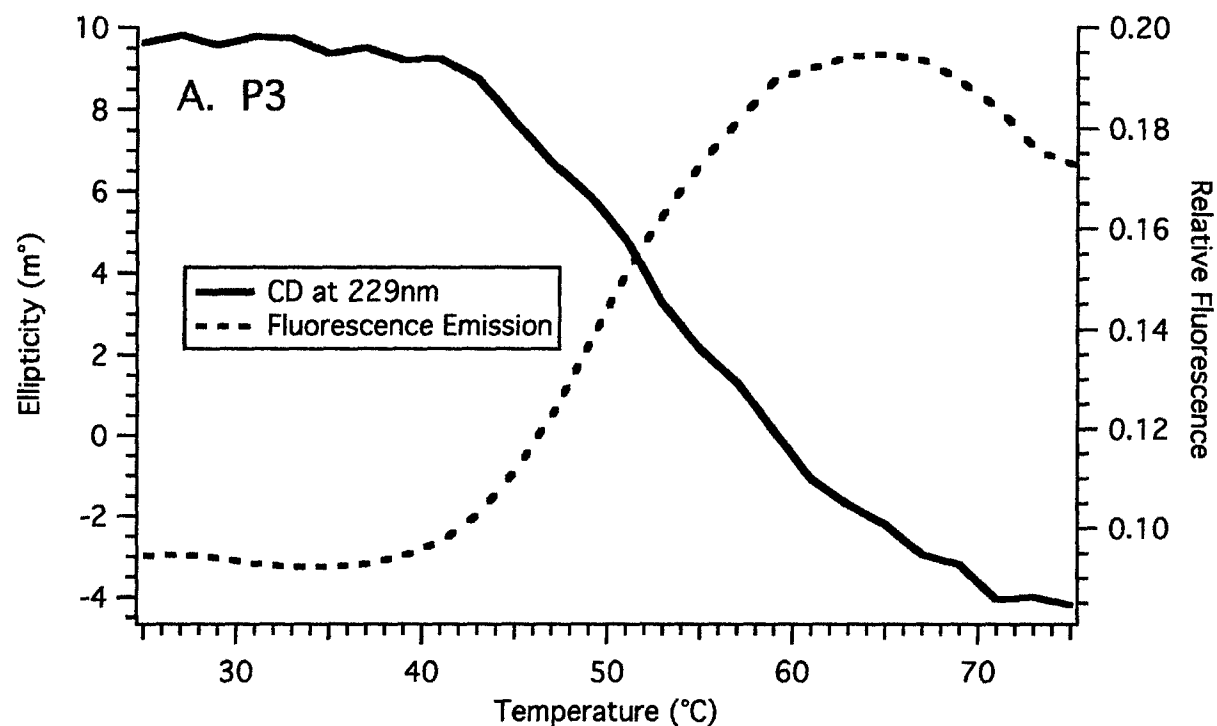
C

Figure 15: Fluorescence Emission Spectra of P3 and P123 under Native and Denaturing Conditions

C
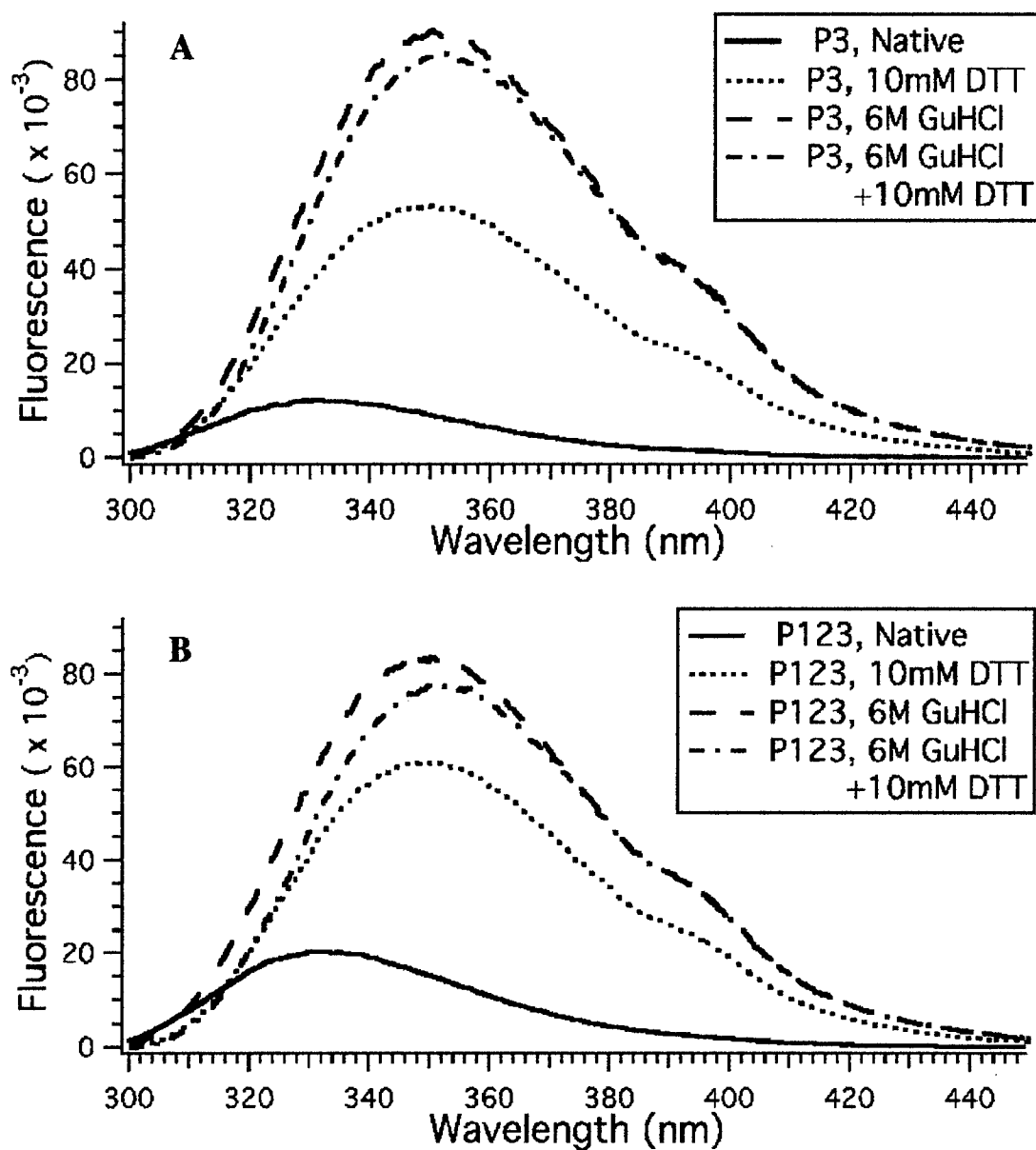
Figure 15: Fluorescence emission Spectra of P3 and P123 under Native and Denaturing Conditions

C. Summary of the Wavelength of Maximum Emission for P3 and P123

Protein	Emission λ_{max}			
	Native	+ 10 mM DTT	+ 6 M GuHCl	+ 6 M GUHCl + 10 mM DTT
P3	332 nm	349 nm	350 nm	352 nm
P123	333 nm	349 nm	347 nm	352 nm

D. Shift in the Wavelength of Maximum Emission Induced by Titration with DTT

C
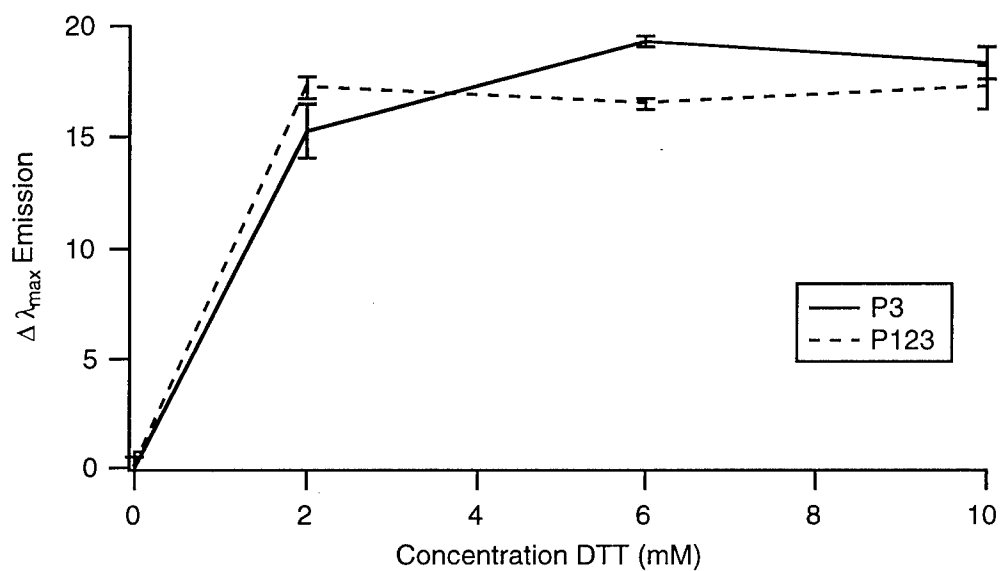
Figure 16: DIG Glycan Western Blot

C
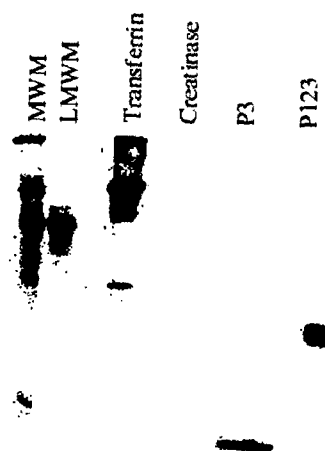
Figure 17:   **Mass Determination of P3 and P123**
                 by MALDI-TOF Mass Spectroscopy

Protein	Average Mass Peak 1	Average Mass Peak 2	Average Mass Peak 3	Average Mass Peak 4
P3	7254.3 Da	7410.4 Da	7562.0 Da	7726.4 Da
P123	19919.0 Da	20077.7 Da		
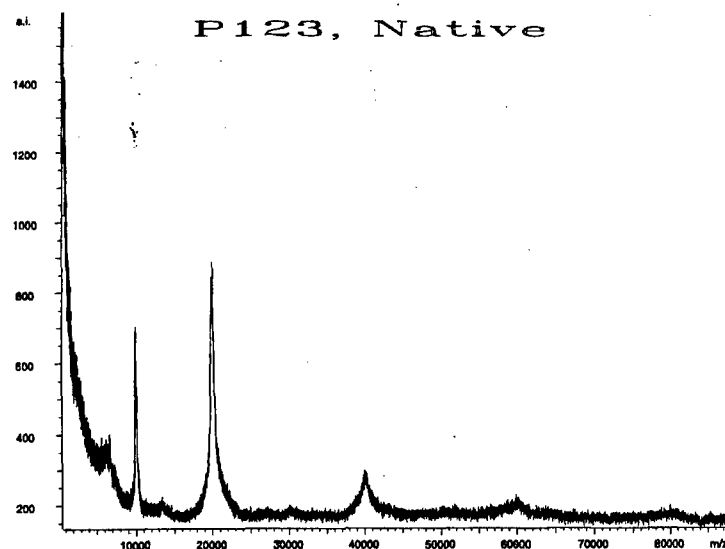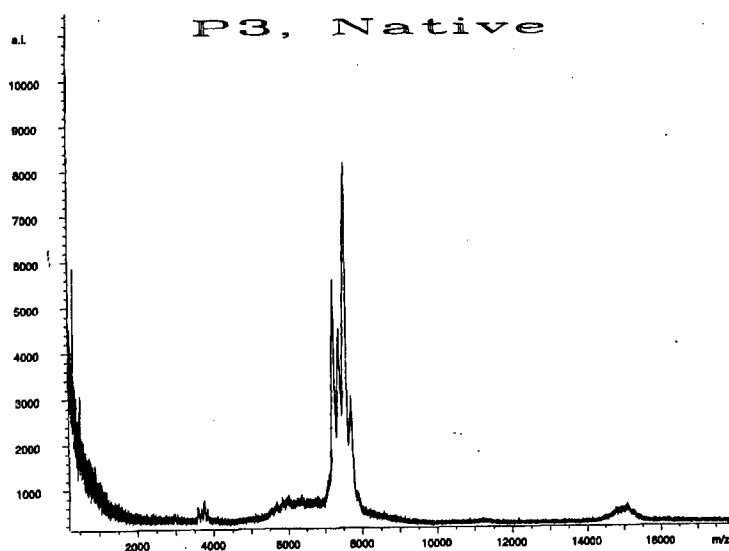
Molecular Mass Determination of P3 and P123 by MALDI-TOF. The data were collected on a Bruker matrix-assisted laser desorption ionization, time-of-flight mass spectrometer. The proteins were dialyzed extensively into 5% acetic acid and then lyophilized. The proteins were resuspended in water to a concentration of 10-40 pmol/ul. The matrix was α-cyano-4-hydroxycinnamic acid at 10mg/ml. Internal calibrants of insulin, ubiquitin, and/or trypsinogen were used to determine the masses. The table lists the average mass determined from several independent experiments. Representative spectra for P3 and P123 without calibrants are also shown.

C

Figure 18: P3 is Disulfide Bonded and Contains No Free Thiols

Treatment	Mass of 1st Peak	ΔMass wrt Native	ΔMass/ Mass IA	Number of Cys Labeled
Native	7246.5 Da	0.0 Da	0.0	0.0
DTT/IA	7597.1 Da	350.6 Da	6.04	6.04
GuHCl/IA	7251.9 Da	5.4 Da	0.09	0.09
DTT/GuHCL/IA	7599.2 Da	352.7 Da	6.08	6.08

Determination of the Disulfide Bond Content of P3 MALDI-TOF. The data were collected on a Bruker matrix-assisted laser desorption ionization, time-of-flight mass spectrometer. The P3 protein was labeled for 30 minutes with Iodoacetic acid (IA) under four conditions: Native; 6mM DTT; 6M Guanidine Hydrochloride; and 6M Guanidine Hydrochloride and 6mM DTT. The protein was equilibrated in each of the four conditions for 90 minutes under nitrogen gas prior to labeling with IA. Following labeling the proteins were dialyzed into 5% acetic acid and then lyophilized. The proteins were resuspended in water to a concentration of 10-20 pmol/ul.

The matrix was α-cyano-4-hydroxycinnamic acid at 10mg/ml. Internal calibrants of insulin and ubiquitin were used to determine the masses. The table lists the mass determined for the first peak of P3 for each treatment condition. The calculated mass difference relative to the first peak of native P3 and the resulting number of Cys labeled by IA are also listed.

C

Figure 19: P3 Expressed in Hi5 and Sf9 Cells
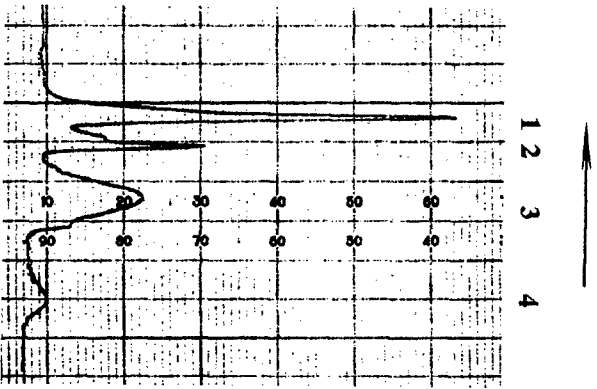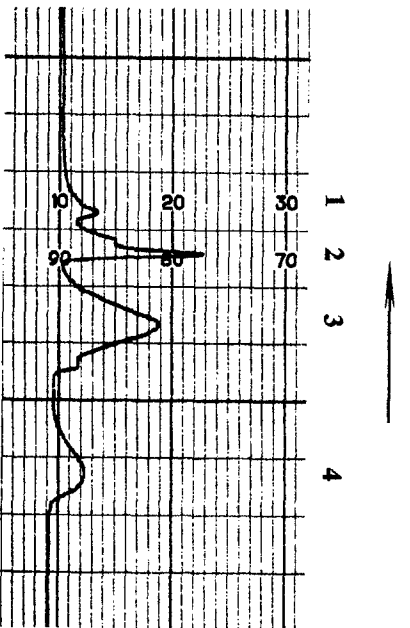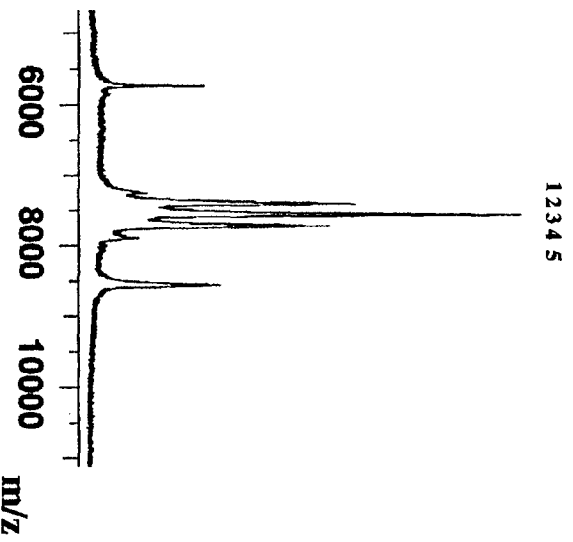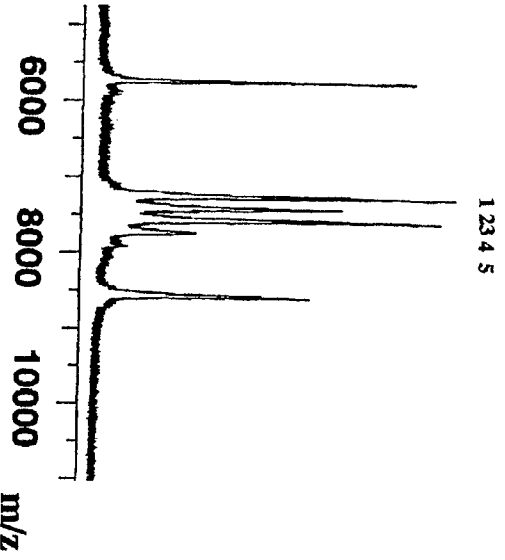
Figure 20: Trypsin Digest of P123 at 37°C

1 2   3   4   5   6   7   8   9   10   11   12   13   14

Reduced   Non-Reduced
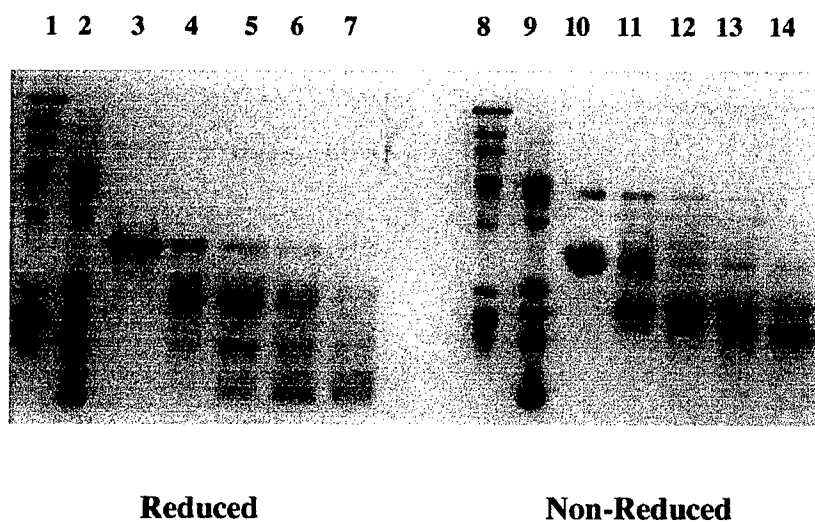
Figure 21: TSP1 induces Cell Death in FBHE seeded on Collagen Gels

C
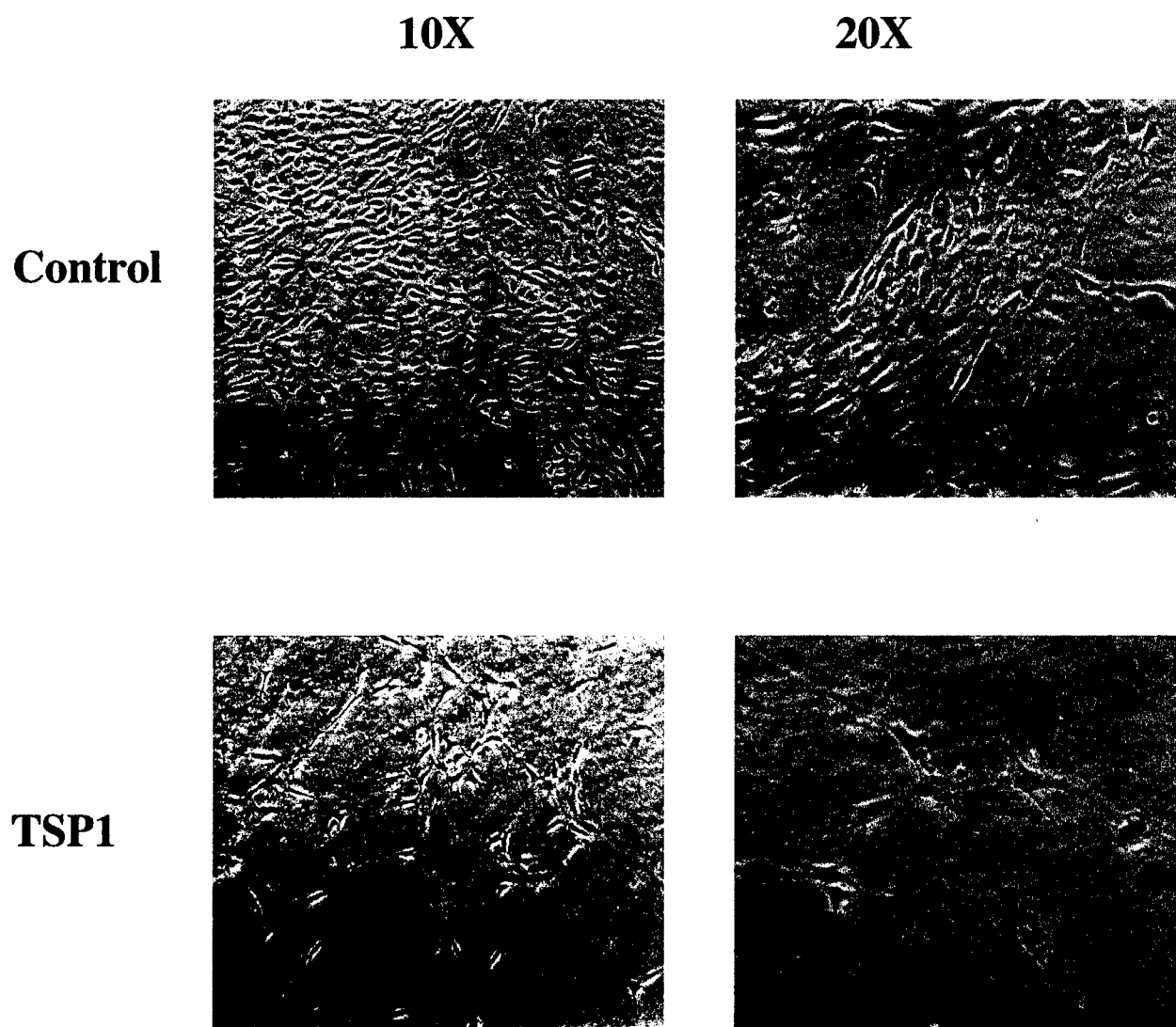
Figure 22: Dose Response of TSP1 (ug/ml) on FBHE seeded on Collagen Gels

C
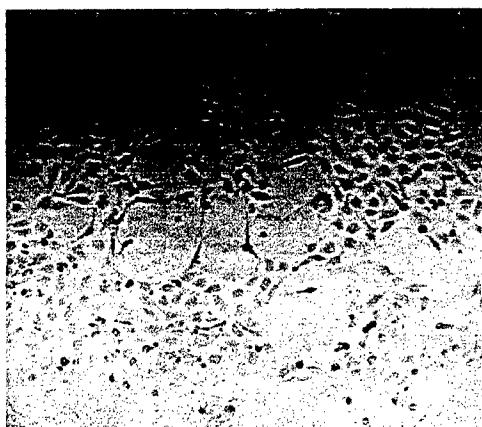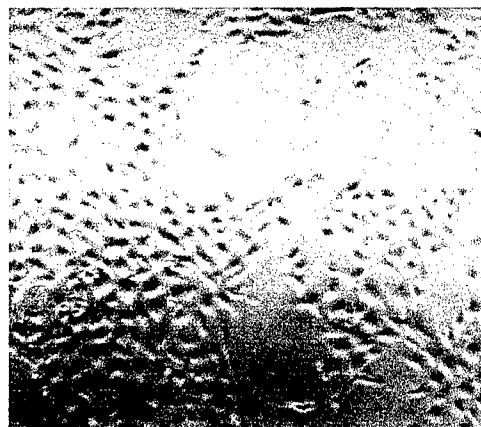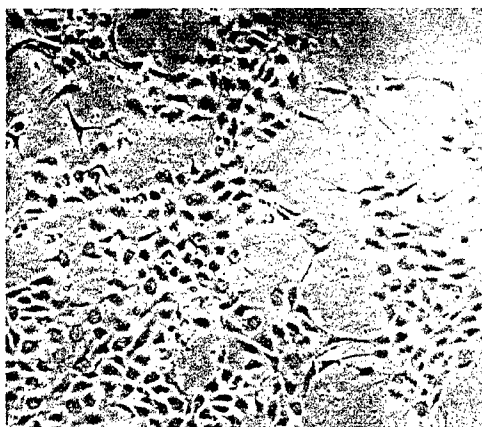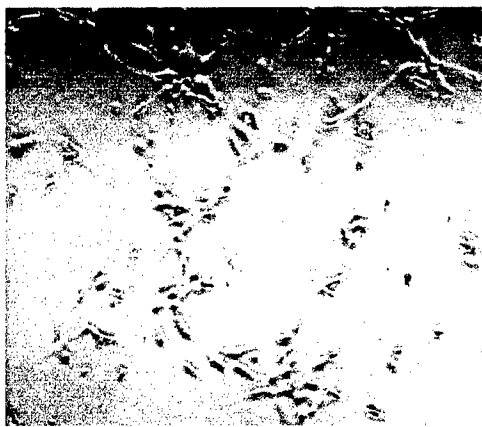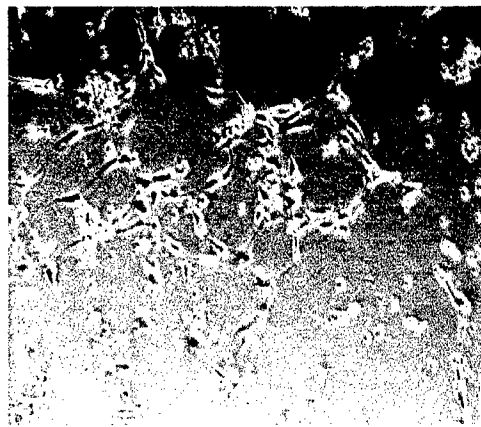
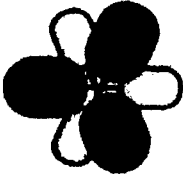# Figure 23: TSP1 induces Nuclear Fragmentation in FBHE
## Seeded on Collagen Gels
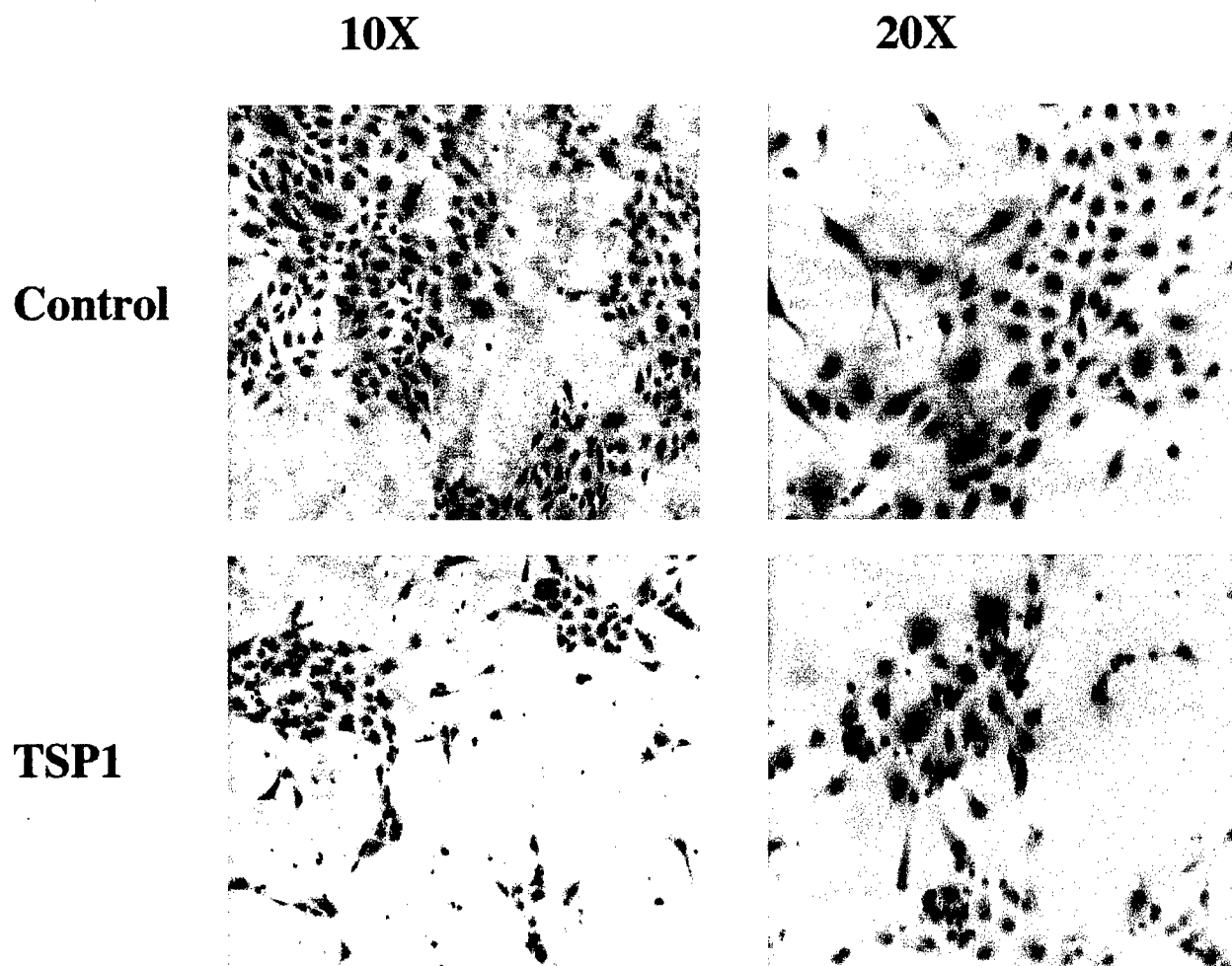
# Figure 24: Recombinant Proteins Expressed using the COCO Baculovirus System

Construct	Calculated Mass	Expression Level
NoC	124.2 kDa	10 mg/L
C	9.4 kDa	25 mg/L
P123	21.3 kDa	20 mg/L
P3	8.5 kDa	1-2 mg/L
CP123	28.3 kDa	10 mg/L
E123	17.6 kDa	40 mg/L
E3	7.0 kDa	10 mg/L
E3Ca1	60.3 kDa	40 mg/L
E3Ca2	60.1 kDa	40 mg/L
delNo1	96.9 kDa	15 mg/L
delNo2	96.9 kDa	5 mg/L

Figure 25: Effect of Recombinant TSP1 fragments on FBHEs Seeded on Collagen Gels
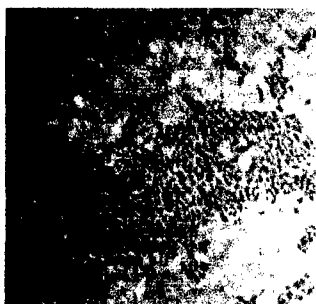

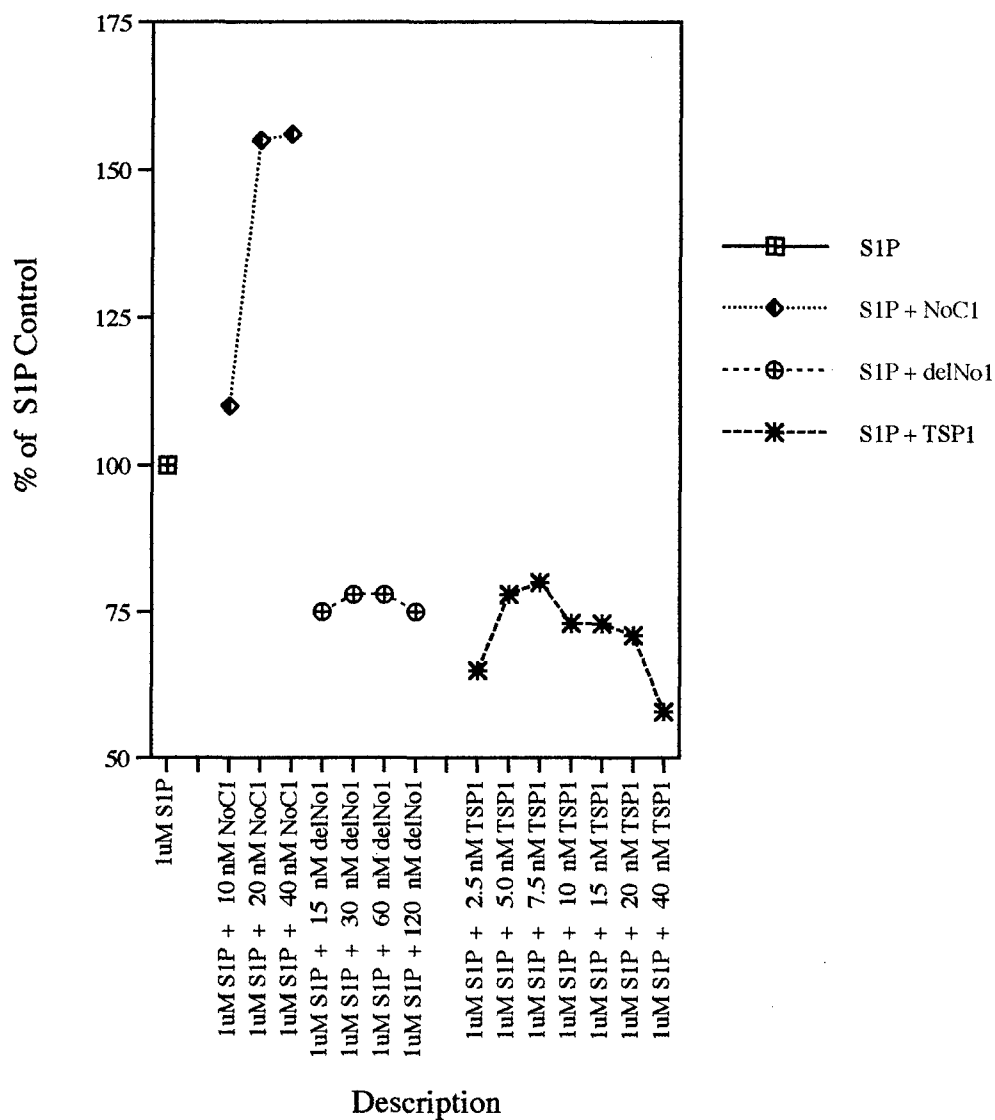Control
(4X)
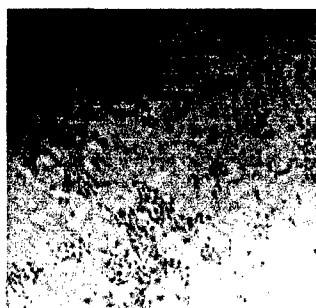
E3Ca1
(4X)

P123
(4X)

P3
(4X)

C
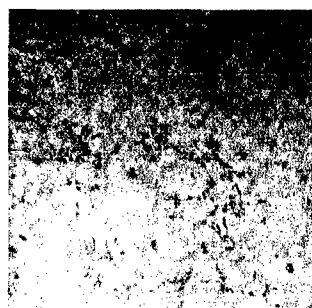
Figure 26: Effect of TSP1 and Recombinant TSP1 Fragments on the Migration of FBHEs in response to S1P

C

XII. Bibliography

A. Personnel supported by grant: Kristin G. Huwiler

B. Meeting Abstracts
1. Genetics, Genomics, and Molecules Symposium   May 23-25, 1999
   Expression of human Thrombospondin 1and 2 Modules:
   Biophysical and Immunological Characterization
   Kristin G. Huwiler, Tina Misenheimer, Douglas Annis, Deane Mosher

The thrombospondin (TSP) gene family consists of five different members that encode secreted modular glycoproteins. TSP1 and TSP2 are disulfide-bonded homo-trimers of approximately 450kDa and are composed of six types of protein modules: N-terminal heparin-binding, oligomerization, procollagen, properdin, EGF-like, and C-terminal calcium binding. TSP1 and 2 are involved in the control of angiogenesis. In order to identify which modules are responsible for this activity, over-lapping segments of the TSPs were recombinantly expressed. The baculovirus expression system was chosen due to its ability to catalyze disulfide bonds and post-translation modifications. The baculoviral transfer vector pAcGP67 was modified 3' to the multi-cloning site by the addition of a DNA sequence that encodes a thrombin cleavage site followed by a series of six His. The resulting vector is named pCOCO. The segments of human TSP1 and 2 cDNA were amplified by PCR and cloned in-frame to the GP67 signal sequence (5') and the cleavable His-tag (3') of pCOCO. The signal sequence directs the recombinant protein for secretion, the His-tag allows its purification from the conditioned media, and cleavage with thrombin allows the removal of the Cterminal His-tag. A multitude of biophysical and immunologic techniques have been employed to characterize the purified recombinant proteins. N-terminal analysis confirmed the homogeneous removal of the signal sequence. Circular Dichroism (CD) in the far-UV was utilized to examine the secondary structure and monitor changess upon thermal denaturation. Near-UV CD and fluorescence spectroscopy studies investigated the chirality and the environment of the aromatic amino acids. Alterations induced by heat, chemical denaturants, and reducing agents were investigated. In addition, the potential involvement of aromatic amino acids in inter-module cross-talk was examined using overlapping recombinant segments. Mass spectroscopy allowed the determination of size, purity, disulfide bond content, microheterogenity, and identification of a novel post-translational modification. HPLC confirmed the purity and presence of microheterogenity. Glycosylation was confirmed by Western blot analysis. ELISA and western blotting allowed precise mapping of antibodies to TSP1 and 2.

2. <u>The 12th Symposium of the Protein Society</u>   July 25-29, 1998

Expression of Characterization of Human Thrombospondin 1 Type 1 Repeats
Krisitn G. Huwiler, Douglas S. Annis, Deane F. Mosher

Thrombospondin 1 (TSP1) is a normal component of the extracellular matrix in many tissues. TSP1 is a disulfide bonded trimer of 450 kD; each monomer contains three type 1 repeats (properdin). TSP1 and TSP1 fragments that include the type 1 repeats cause an endothelial cell-specific inhibition of growth and migration. The type 1 repeats were expressed using the baculovirus protein expression system. The baculovirus transfer vector pACGP67 was modified 3' to the multi-cloning site (MCS) by the addition of a DNA sequence that encodes a thrombin cleavage site followed by a series of six His (pCOCO). The cDNAs encoding the three type 1 repeats in tandem (P123) and the third type 1 repeat (P3) were cloned separately into the MCS of pCOCO. N-terminal sequencing of P123 and P3 confirmed that the GP67 signal sequence, which directs the secretion of these recombinant proteins, was removed. The third type 1 repeat contains a consensus site for N-linked glycosylation, and both P123 and P3 have carbohydrate. Each type 1 repeat contains a distinctive set of conserved residues- three Trp, two Arg, six half-Cys, and no Tyr. The far-UV CD spectra for P3 and P123 are marked by distinctive positive ellipticity that is lost by thermal denaturation. The near-UV CD spectra are positive and upon heating approach zero ellipticity. Either 6M guanidine hydrochloride or 10 mM DTT caused a major change in Trp fluorescence, with red shift of maximum emission from 332nm to 350nm and a several-fold increase in fluorescence intensity. These results indicate that the type 1 repeat encodes an independently folding protein module with spectral properties dominated by the conserved Trp.

MCMR-RMI-S   (70-1y)   19 Jan 01

MEMORANDUM FOR Administrator, Defense Technical Information
               Center, ATTN: DTIC-OCA, 8725 John J. Kingman
               Road, Fort Belvoir, VA 22060-6218

SUBJECT: Request Change in Distribution Statement

1. The U.S. Army Medical Research and Materiel Command has
reexamined the need for the limitation assigned to technical
reports written for Grant DAMD17-96-1-6151. Request the limited
distribution statement for Accession Document Number ADB255411 be
changed to "Approved for public release; distribution unlimited."
This report should be released to the National Technical
Information Service.

2. Point of contact for this request is Ms. Judy Pawlus at
DSN 343-7322 or by email at judy.pawlus@det.amedd.army.mil.

FOR THE COMMANDER:

                              PHYLIS M. RINEHART
                              Deputy Chief of Staff for
                                 Information Management